

MAPPING CARBON STOCK USING HIGH RESOLUTION SATELLITE IMAGES IN SUB- TROPICAL FOREST OF NEPAL

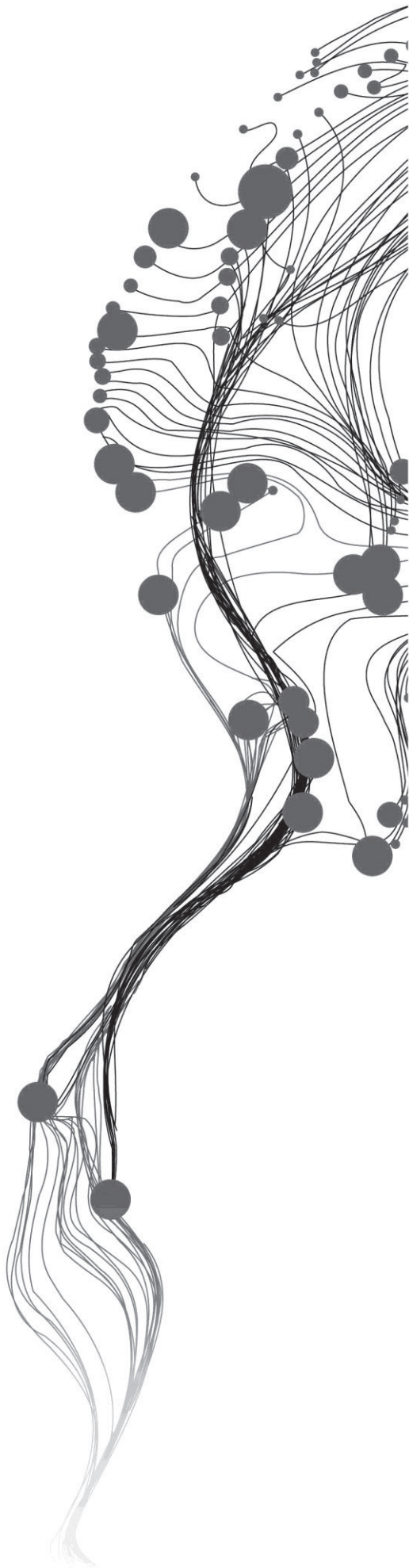
SRIJANA BARAL

February, 2011

SUPERVISORS:

Ms. Ir, L.M. Leeuwen

Dr. Y.A, Hussin



MAPPING CARBON STOCK USING HIGH RESOLUTION SATELLITE IMAGES IN SUB- TROPICAL FOREST OF NEPAL

SRIJANA BARAL

Enschede, The Netherlands, [February, 2011]

Thesis submitted to the Faculty of Geo-Information Science and Earth Observation of the University of Twente in partial fulfilment of the requirements for the degree of Master of Science in Geo-information Science and Earth Observation.

Specialization: Natural Resource Management

SUPERVISORS:

Ms. Ir, L.M. van Leeuwen

Dr. Y.A. Hussin

THESIS ASSESSMENT BOARD:

Prof. Dr. A. Skidmore (Chair)

Dr. Ir. J.G.P.W. Clevers (External Examiner, Laboratory of Geo-Information Science and Remote Sensing, Wageningen)

DISCLAIMER

This document describes work undertaken as part of a programme of study at the Faculty of Geo-Information Science and Earth Observation of the University of Twente. All views and opinions expressed therein remain the sole responsibility of the author, and do not necessarily represent those of the Faculty.

ABSTRACT

Estimation of above ground carbon stock is essential for understanding the global carbon cycle. All countries committed to UNFCCC and Kyoto Protocol and participating in REDD should update the inventories of emissions of greenhouse gases and estimate the amount of carbon stock. But accurate carbon stock mapping from satellite imagery is still a challenge. Thus, this study aims to develop a method to estimate amount of above ground carbon stock in the natural sub-tropical forest of Chitwan, Nepal using high resolution satellite images.

Geo-Eye and Worldview, very high resolution images were used for the study. Both the images have same spatial resolution but have difference in spectral resolution. Total above ground biomass (AGB) is estimated using allometric equation from the DBH measured in the field, which was then converted to carbon stock using a conversion factor. The relationship between crown projection area (CPA) and Carbon was established using carbon stock of 78 trees recognized in the field and CPA derived from image. Object based image analysis was carried out in both the images to obtain CPA. A non-linear regression model was developed between the calculated carbon and CPA derived from image to estimate image carbon stock in the study area. The estimated carbon stock was validated using validation data set collected in field.

The segmentation and classification results were better in case of Geo-Eye compared to Worldview. Classification was done in two classes with *Shorea robusta* and other species. So, CPA derived from Geo-Eye was used to develop a non-linear regression model to produce a carbon map. The regression model developed was significant and yield high coefficient of determination in both the classes. The model was applied to obtain carbon map with carbon stock approximately 70 MgCha⁻¹. Non-linear model explained 61% of the predicted carbon. Shadow content, use of general allometric equation and time lag in data collection and image acquisition, high solar angle *etc.* are the sources of error in carbon stock estimation. Thus, carbon stock mapping in subtropical forest is feasible using high resolution satellite images.

Keywords: Object based image analysis, Segmentation, Classification, Carbon Stock, Allometric equation, Regression

ACKNOWLEDGEMENTS

I would like to take this opportunity to thank all the special people and organizations whose efforts and contributions are valuable for me to accomplish my study in Faculty of Geo-Information and Earth Science (ITC), University Twente. This has been a major achievement of my life.

First and foremost I would like to express my sincere gratitude and appreciation to my supervisor, Ms. Ir. L.M. Louise van Leeuwen for her creative guidance, constructive feedback and comments and words of encouragement from the very beginning till the completion of this research and for bringing ideas to shape up my work. Thanks goes to my second supervisor Dr. Yousif Hussin whose critical suggestions and continuous support to me from inception till the end and the inspirations have added strength in me.

My deepest appreciation goes to Prof. Dr. Andrew Skidmore for his comments and suggestions during my proposal and mid-term defence, which has added flavour in my research.

I'm greatly indebted to Dr. Michael Weir, Course Director, NRM, for his support, advice and guidance during my study. I'm also thankful to NRM department faculty members who always supported my study.

I would like to acknowledge the sponsorship I received from the Government of the Netherlands under Netherlands Fellowship Programme (NFP) to make my dream come true. Thanks goes to ICIMOD and ANSAB team for their support during the fieldwork and other technical support. My appreciation goes to the people of Shaktikhor VDC, Chitwan, Nepal for their support and hospitality during the fieldwork.

Special thanks to my Nepali classmates Upama, Rachna, Saurav, Sahash and Shyam who were always there for me in my hard times and your willingness to help each other during the research period is highly appreciated. Thanks to my Nepali mates for your support and encouragements. You guys always made me feel at home. My appreciation to all NRM batch 2009-2011, we always enjoyed our life together. Special thanks to Nandika, Dinesh and Jiwan who were always there beside me during those hard times in core modules and till the end of my studies.

Finally, I'm indebted to my family and want to dedicate my thesis to my cute little children Sarthak and Sarvashree who sacrificed so much to let their mom study and my beloved husband JK for his patience and support during my study, to my dad - mom for being the source of inspiration throughout my life, my parents in law Mr & Mrs Jamarkattel, who always supported me in each step I took, my brother Gaurav and sisters Anjana and Bimla for caring and loving me so much.

Srijana Baral

Enschede, The Netherlands

February, 2011

... "dedicated to my Parents, my love JK and my lovely children Sarthak and Sarvashree"

TABLE OF CONTENTS

Abstract	1
Acknowledgements	2
List of Figures.....	4
List of Tables.....	5
List of Appendixes.....	6
List of Acronyms	7
1. Introduction.....	1
1.1. Background	1
1.2. Community forest (CF) in Nepal	2
1.3. Overview of tools and techniques for biomass estimation	3
1.4. Object based image analysis for carbon stock estimation	4
1.5. Rationale and problem description	5
1.6. Objectives.....	7
1.7. Theoretical Framework of research	8
1.8. Concepts and definitions	9
1.8.1. Biomass and Carbon.....	9
1.8.2. Crown Projection Area	9
1.8.3. Allometric Equation	9
1.8.4. Object Based Image Classification.....	10
1.8.5. Community Forest.....	10
2. Study Area.....	11
2.1. Criteria for study area selection.....	11
2.2. Overview of Chitwan district	11
2.2.1. Land use	11
2.2.2. Social, economic and demographic.....	11
2.2.3. Climate.....	11
2.2.4. Vegetation	12
2.2.5. Kayerkhola watershed area.....	12
3. Materials and Methods.....	13
3.1. Data used.....	13
3.1.1. Satellite data	13
3.1.2. Maps.....	13
3.1.3. Software.....	13
3.1.4. Filed equipment.....	14
3.2. Image pre-processing.....	14

3.2.1.	Image mosaic and subset.....	14
3.2.2.	Image fusion.....	14
3.2.3.	Image filtering/Convolution.....	15
3.3.	Research Method	16
3.4.	Field work	17
3.4.1.	Sampling design	17
3.4.2.	Data collection from field work.....	17
3.4.3.	Sampling Plots.....	17
3.5.	Field work data analysis	18
3.5.1.	Manual delineation of tress	18
3.6.	Segmentation of images	18
3.6.1.	Multi-resolution segmentation.....	18
3.6.2.	Scale parameter	19
3.6.3.	Estimation of Scale parameter.....	20
3.7.	Procedure of Segmentation.....	20
3.7.1.	Pre-processing in eCognition.....	22
3.7.2.	Masking out shadow and cloud.....	22
3.7.3.	Parameters Setting using ESP.....	22
3.7.4.	Watershed transformation.....	22
3.7.5.	Morphology	22
3.7.6.	Removal of some undesired objects.....	23
3.8.	Segmentation validation.....	23
3.9.	Image classification and accuracy assessment	23
3.9.1.	Transformed divergence (D_T).....	23
3.9.2.	Image classification.....	24
3.9.3.	Accuracy Assessment.....	24
3.10.	Above Ground Biomass and Carbon Stock calculation.....	24
3.11.	Regression Ananlysis and validation of the model.....	25
4.	Results.....	27
4.1.	Image segmentation.....	27
4.1.1.	Estimation of Scale Parameter.....	27
4.1.2.	Multi-resolution segmentation.....	27
4.1.3.	Segmentation accuracy.....	28
4.2.	Image classification.....	29
4.2.1.	Transformed divergence.....	29
4.2.2.	Spectral means of the classes in every band	30

4.2.3.	Classification accuracy of Geo-eye.....	31
4.2.4.	Classification accuracy of Worldview-2 image.....	32
4.3.	Descriptive Statistics.....	35
4.4.	Model development and validation.....	36
4.4.1.	Relationship between CPA and Carbon of <i>Shorea robusta</i>	36
4.4.2.	Relationship between CPA and Carbon of other species	37
4.4.3.	Model validation.....	38
4.5.	Carbon Stock mapping.....	39
5.	Discussion.....	41
5.1.	Image segmentation and accuracy assessment	41
5.2.	Image classification using Geo-Eye and Worldview-2 images	41
5.2.1.	Probable reasons for low segmentation and classification accuracy of worldview images	42
5.3.	Model Development.....	43
5.4.	Biomass and Carbon stock estimation.....	44
5.5.	Sources of error or uncertainties	44
5.5.1.	Shadows causing error in f high resolution satellite images.....	44
5.5.2.	Allometric equations.....	45
5.5.3.	Time of image acquisition	46
5.6.	Limitations of the research.....	46
5.6.1.	Intermingling situation in the natural forest.....	46
5.6.2.	Sampling design.....	46
5.6.3.	Undergrowth not addressed by the model	46
6.	Conclusion and Recommendations	47
6.1.	Conclusions.....	47
6.2.	Recommendations.....	48
	List of references	49
	Appendices	55

LIST OF FIGURES

Figure 1: Theoretical framework of thesis	8
Figure 2: Biomass of a tree, Source: (Gschwantner, <i>et al.</i> , 2009).....	9
Figure 3: Crown Projection Area, Source: (Gschwantner, <i>et al.</i> , 2009).....	10
Figure 4: Location of study area, Chitwan, Nepal.....	12
Figure 5: Methods Flow Chart	16
Figure 6: Multi-resolution segmentation concepts flow.....	19
Figure 7: ESP tool for determining scale.....	20
Figure 8: Segmentation process	21
Figure 9: 3D view of the Geo-Eye image.....	21
Figure 10: After (Zhan, <i>et al.</i> , 2005) showing different conditions of one to one matching.....	23
Figure 11: ESP tool of Geo-Eye and Worldview-2 images.....	27
Figure 12: Multi-resolution segmentation of Geo-Eye image (Green colour lines showing trees and brown colour lines showing shadow region)	28
Figure 13: Visual evaluation of manual segments versus automatic segmentation of Geo-Eye image.....	29
Figure 14: Fused Geo-Eye image (Inset: zooming into tree level).....	29
Figure 15: Spectral separability of species using GeoEye image	31
Figure 16: Spectral separability of species using Worldview image.....	31
Figure 17: Classified map of Geo-Eye image	33
Figure 18: Classified map using Worldview	34
Figure 19: Species composition in the study area	35
Figure 20: Box plot of the DBH of the trees measured in the field.	36
Figure 21: Graph showing the non-linear relationship between CPA and Carbon.....	37
Figure 22: Scatter plot of non-linear relationship between CPA and Carbon of Other species	38
Figure 23: Scatter plot of model validation of <i>Shorea robusta</i>	38
Figure 24: Scatter Plot of model validation for other species	39
Figure 25: Carbon stock map of the study area and the inset shows the details of carbon stock per tree crown.....	39
Figure 26: a) Worldview image with cloud and lot of cloud shadow b) Distortion in Worldview image.....	43
Figure 27: Missing pixels of a tree because of shadow.....	45

LIST OF TABLES

Table 1: Research Objective, research questions and hypothesis	7
Table 2: Software used in the research.....	13
Table 3: Field equipment used for the study.....	14
Table 4: "D" value of different segmentation scales as determined in Figure 12.....	28
Table 5: Matching 1 to 1 relation of the segmented CPA with the reference CPA.....	28
Table 6: Transformed divergence of Geo-Eye image.....	30
Table 7: Transformed divergence of Worldview image	30
Table 8: Accuracy assessment of classification with two species using Geo-Eye image	32
Table 9: Accuracy assessment of classification with two classes in Worldview	32
Table 10: Forest inventory	35
Table 11: Regression Analysis of <i>Shorea robusta</i>	36
Table 12: ANOVA test results of other species	36
Table 13: Non-Linear Regression analysis of other species.....	37
Table 14: ANOVA test results of other species	37

LIST OF APPENDIXES

Appendix 1: Specification of the images used	55
Appendix 2: Data collection format.....	56
Appendix 3: Map of the sample plot used for tree identification in the field	57
Appendix 4: Sample plots	58
Appendix 5: List of tree species in the study area.....	59
Appendix 6: Glimpse of the Chitwan	60

LIST OF ACRONYMS

AGB	Above ground biomass
ANSAB	Asia Network for Sustainable Agriculture and Bio-resources
CF	Community Forest
CFUGs	Community forest user groups
CO ₂	Carbon dioxide
CPA	Crown projection area
DBH	Diameter at base height
DN	Digital number
FAO	Food Agricultural Organization
GHG's	Greenhouse gases
GPS	Global Positioning System
ICIMOD	International Centre for Integrated Mountain Development
IPCC	International Panel on Climate Change
IR	Infra red
ITC	Individual tree crown
MOFSC	Ministry of Forest and Soil Conservation
OBIA	Object based image analysis
REDD	Reducing Emission from Deforestation and Degradation
RMSE	Root Mean Square Error
D _T	Transformed divergence
UNFCCC	United Nations framework Convention on Climate Change

1. INTRODUCTION

1.1. Background

Forest with its key carbon function has a crucial role in the global agenda of climate change. Healthy forests sequester and store more carbon compared to other terrestrial ecosystems and are considered to be an important natural brake on climate change (Gibbs, *et al.*, 2007). Currently world's forests and forest soils store more than one trillion tons of carbon, which is twice the amount found floating free in the atmosphere (FAO, 2008). However, forest biomass can act as both source and sink. When the forest is healthy and growing, carbon is sequestered in atmosphere but when the forests are destroyed, overharvested, or burned, they no longer contribute in sequestration but become source of CO₂ and enhancing climate change. Hence, reforestation, afforestation and avoiding deforestation are mechanisms of tackling climate change (Hunt, 2009).

Forest carbon financing, both through the compliance market (Kyoto Protocol) as well as voluntary market has gained a wider attention these days. United Nations Framework Convention on Climate Change (UNFCCC) on 11 December 1997 adopted Kyoto Protocol (UNFCCC, 2011), which sets binding targets to industrialized countries for reducing GHGs emissions. The Bali Action Plan Conference of the Parties (COP-13) in 2007 opened windows of opportunities for developing countries to participate in forest carbon financing through the mechanism of reducing emissions from deforestation and forest degradation (REDD) (MOFSC, 2009). In fact, REDD is a win-win strategy whereby host countries *i.e.* the developing countries can be compensated for the use of land for forest and planting trees, while industrialized countries are expected to pay for the carbon credits (Dhital, 2009). The essence is that industrialised countries have to compensate for their emissions and can do so by paying for reforestation. Emissions are converted to carbon credits in the carbon trade. All the greenhouse gas inventories and emissions reduction programs require scientifically robust methods to quantify forest carbon storage over time across extensive landscapes (Gonzalez, *et al.*, 2010). Nepal being a UNFCCC signatory has been participating in REDD as a potential member of carbon trade, which requires estimation of carbon stock in the country to be prepared for REDD implementation.

Carbon is 47% of the Above Ground Biomass (AGB) which is defined as “all biomass of living vegetation, both woody and herbaceous, above the soil including stems, stumps, branches, bark, seeds, and foliage” (IPCC, 2007b). Forest inventories and remote sensing (RS) are the two principal data sources used to estimate AGB (Krankina, *et al.*, 2004) and hence ultimately carbon stocks. A common practice is to develop a statistical relationship between ground based measurements and satellite imagery (Gibbs & Herold, 2007) to estimate carbon stock. Various types of satellite images are used to map the carbon (Thenkabail, *et al.*, 2004).

High resolution satellite remote sensing has been a very useful source of data (Nagendra & Rocchini, 2008) and in forestry context the trend of using high resolution satellite imagery like Geo-Eye, Worldview-2, IKONOS and Quick bird for carbon mapping is becoming common for achieving precise results (Gonzalez, *et al.*, 2010). High resolution satellite images has been used in recognizing individual trees and vegetation types (Wulder, 2004; Hall, *et al.*, 2004) and extraction of forest inventory information (Chubey, *et al.*, 2006). But extraction of forest information from high resolution satellite images has increased the

challenge to develop a new interpretation procedure (Culvenor, 2003). Thus, object based image analysis is being used to analyse these high resolution satellite images

Object based image analysis (OBIA) has been used to improve the accuracy of forest biomass estimation by combining pixel information with the object characteristics. It is efficient in using automated image segmentation to extract meaningful ground features from imagery. The approach is valuable in segmenting an area consisting of various land cover types into objects with similar properties (Lamonaca, *et al.*, 2008). In fact, Morales, *et al.*, (2008) found that the segmentation technique was effective in differentiating tree crown from objects of similar reflectance and size in Hawaiian forest. Similarly, Chubey, *et al.* (2006) observed strongest relationship between land-cover types, species classification, and crown closure using high resolution satellite image and object based image classification. These object based methods are more effective in classification of the high resolution images. Hence object based image analysis software such as eCognition deserves explicit mention in a forestry context (Pekkarinen & Holopainen, 2006) and has provided acceptable results in extraction of forest inventory parameters.

Forests cover nearly 40% of the total land area of Nepal (Oli & Shrestha, 2009) which signifies the amount of carbon in the forests of Nepal. But national forest inventory data on changes in forest cover, biomass stocks, carbon emissions and carbon removals on a periodic basis are limited (Acharya, *et al.*, 2009). In order to capture the benefits accruing from climate change scenario, there is an urgent need of obtaining reliable baseline statistics on carbon stocks and fluxes in forest which requires advanced remote sensing technologies (Oli & Shrestha, 2009). In addition, carbon credit buyers will expect the use of a robust methodology of carbon accounting and monitoring (Acharya, *et al.*, 2009) while commencing carbon trade. Hence, it becomes crucial to produce a credible estimate of national forest carbon stocks and sources of carbon emissions, to determine a national reference scenario and develop a national REDD strategy in Nepal (MOFSC, 2009).

1.2. Community forest (CF) in Nepal

Nepal is acknowledged and highly appreciated for its participatory forest management regimes. Currently Community Forest, Collaborative Forest, Leasehold Forest, Religious Forest, Protected Forest and Government Managed Forest are the different types of forest management regimes existing in Nepal. Amongst all the regimes, Community Forestry program in Nepal is a participatory forest management that encompasses well-defined policies, institutions, and practices (Ojha, *et al.*, 2009).

The forests of Nepal have been handed over to the local communities since the 1970's and this is further facilitated by Forest Act of 1992 and Forest Rules of 1995. Community forest is National forest handed over to a community forest user group (CFUG) for its development, conservation and utilization (FAO, 2010). CFUGs are autonomous and perpetual institutions with rights to mobilise all types of resources to ensure the wellbeing of communities at large. In practice, these CFUGs of Nepal are conducting a range of community development activities (Chapagain & Banjade, 2009)

The Community Forestry programme is regarded to be successful not only in increasing the plantation of degraded sites, biodiversity, improving the supply of forest products to rural people but also in forming local level institutions for resource management and in improving the environmental situation in the hills of Nepal (Acharya, 2002). Apart from these, community forests in Nepal has been involved in different types of community development works which is a result of the voluntary involvement of CFUGs in the management of forest resources (Acharya, 2002). Thus, CF programme is a popular forest management

regime in Nepal. Due to its popularity, one-third of country's population was practicing CF and directly managing over one-fourth of Nepal's forest area (Ojha, *et al.*, 2009) till April 2009.

1.3. Overview of tools and techniques for biomass estimation

Forest biomass is the total amount of above ground living organic matter contained in a tree which is expressed as oven-dry tons per unit area. Carbon is derived from above-ground biomass using a conversion factor, Carbon is regarded as 47% of dry weight of above ground biomass (IPCC, 2007a). In some literatures the carbon is taken to be 50% of AGB (Andersson, *et al.*, 2009; Basuki, *et al.*, 2009).

There are different approaches, tools and techniques for biomass estimation. Lu, (2006) reviewed and summarized different approaches of biomass estimation methods based on field measurements; remote sensing and GIS based methods. Field based conventional method, of harvesting and weighing the biomass is the most accurate (Greenberg, *et al.*, 2005; Lu, 2006), but this method requires hard-work, it is time consuming, destructive and biased for dry weight estimation and also inappropriate for large scale biomass estimation (Greenberg, *et al.*, 2005). In short, this method is not practical for global or regional biomass estimation (Andersson, *et al.*, 2009). GIS based method is extrapolation of existing forest inventory volume data to biomass estimation using wood density. But it has limitations of having difficulty in obtaining good quality forest inventory data, another drawback for this method is that branch wood is not normally included in forest inventory and also wood density of particular species varies according to location and even within each tree (Faganaa & DeFries, 2009) which is required for biomass estimation. In remote sensing based method, statistical relationship between satellite extracted tree parameters and ground based measurements is used in biomass estimation (Gibbs, *et al.*, 2007). The reasons for using remote sensing is that it is cost effective in assessing large spatial extents (Andersson, *et al.*, 2009), hence it is a popular method and widely used for biomass estimation.

In spite of technological advancements, it is not possible to directly measure biomass of the forest (Andersson, *et al.*, 2009; Gibbs, *et al.*, 2007; Rosenqvist, *et al.*, 2003) but the reflectance from the forest can be related to biomass estimates based allometric equations obtained from field measurement (IPCC, 2007a; Patenaude, *et al.*, 2005; Rosenqvist, *et al.*, 2003). These allometric equations are the most accurate when species and region specific but general equation is also used with reasonable results. Different remote sensing sensors are used for biomass estimation. Coarse resolution pixels usually receive response from several stands, which makes the direct biomass estimation problematic (Muukkonen & Heiskanen, 2007) and tends to underestimate carbon stock. Medium resolution satellite image *e.g.* Landsat have become the primary source of data in many application including AGB estimation (Lu, 2006). But estimation of AGB using these data is limited because of the mixed pixels (Muukkonen & Heiskanen, 2007). Steininger,(2000) faced problem of data saturation while estimating AGB in tropical regenerating forest using medium resolution Landsat TM data. These sensors can only provide proportional estimates of woody cover and cannot be used for analyzing tree cluster patterns (Boggs, 2010). Apart from this, these coarse resolution satellite image data cannot be interpreted either visually or automatically to derive individual tree crowns (Hirata, 2008). In this regard, medium spatial resolution satellite remote sensing data such as Landsat Thematic Mapper and SPOT are insufficient for stand-level analysis (Ke, *et al.*, 2010) which is substantiated by high resolution satellite images. In general, medium resolution images are well suited for the land classification, while fine resolution images are better adapted for measuring forest variable inputs for the allometric models (Andersson, *et al.*, 2009).

Apart from optical remote sensing, Radar (Radio Detection and Ranging) has been frequently used in biomass estimation. It uses the microwaves energy and captures the backscatter from the object. It has the

ability to penetrate the clouds, but while working in the dense tropical forest even in long wavelength bands, having capability to penetrate the tree canopy also suffers as the sensitivity of radar backscatter saturation (Greenberg, *et al.*, 2005) for example, world's largest white fir has biomass of 5421. Mgha⁻¹ while the upper limit of the biomass that can be estimated by Radar is about 360 Mgha⁻¹ (Kasischke, *et al.*, 1997).

Optical remote sensing has a limitation of producing 2-dimensional images as it cannot fully represent the 3-dimensional spatial features of forests. Three dimensional features are taken into consideration by LiDAR (Light Detection and Ranging) (Omasa, *et al.*, 2003). LiDAR does not penetrate clouds but has the unique capability of measuring the three-dimensional vertical structure of vegetation in great detail which in itself is an advantage over high resolution satellite imagery (Song, *et al.*, 2010). Lidar instruments have demonstrated the capability to accurately estimate forest structural characteristics such as canopy heights, stand volume, basal area and aboveground biomass (Dubayah & Drake, 2000). In spite of these advantages, LiDAR data are extremely expensive are not yet available from satellite platforms (Patenaude, *et al.*, 2005) which limits their usefulness to only highly localised analysis (Greenberg, *et al.*, 2005).

In the recent years very high resolution (VHR) satellites have been launched. The launch of the first commercial satellite with a resolution of less than a half a meter Worldview-1 in 2007 (Blaschke, 2010) there after followed by other commercial high resolution satellites like Geo-Eye, IKONOS, Worldview and others have provided opportunity to the technology to even identify a single object. Geo-Eye image with 50 cm panchromatic and four multispectral bands have added flavour to the image analysis and classification. Use of high resolution images has been blamed for having the disadvantage of low spectral resolution which has been demolished by the launch of eight band multispectral Worldview-2. Worldview-2 is said to be the second generation satellite having a unique combination of various bands (DigitalGlobe, 2009). The spectral coverage of bands is two bands of blue *i.e.* blue and coastal blue, followed by green, yellow, red, red edge and two bands of Near Infrared (DigitalGlobe, 2009). The yellow, Red-edge and two bands of NIR are regarded important for vegetation study. These high resolution images now provide new opportunities to develop detailed forest inventories techniques (Morales, *et al.*, 2008).

Using these high resolution images with spatial resolution of less than 5m (Lu, 2006) it is possible to recognize, identify and delineate individual tree crown (Gougeon & Leckie, 2006). Various operations like tree quantification, tree crown delineation, species identification, crown density estimation, and forest stand polygon delineation have been conducted with high-resolution data (Katoh, *et al.*, 2009). However these high resolution images do not necessarily provide better classification of the image (Carleer, *et al.*, 2005) using pixel based classification as pixels in this type of images are far smaller than the object. So, a different approach is required to analyse the very high resolution images, and OBIA has emerged as an alternative to the traditional pixel-based paradigm (Castilla & Hay, 2008).

1.4. Object based image analysis for carbon stock estimation

The high resolution satellite images brought about paradigm shift in image analysis procedure. This approach is different from traditional pixel-based classification methods as only pixels spectral information is used to extract surface features which cannot satisfy high-resolution image classification precision and produce large data redundancy (Wei, *et al.*, 2005). So, to process VHR images OBIA is regarded as an ideal approach as it can incorporate information on spatial extent (Zhang, *et al.*, 2010). Various studies have been conducted to investigate the relevancy of object based image analysis. Heyman *et al.* (2003) favoured an OBIA approach to discriminate broad-scale forest cover types. Hay, *et al.*, (2005)

studied about how segments correspond to individual tree crowns, using segmentation and object specific analysis.

With the availability of high resolution satellite images, there are emergence of different options for delineating individual crowns and identifying the crowns at species level but studies on these automated techniques yet remains as the field of research (Bunting, *et al.*, 2010). The object-based information extraction with eCognition software provides a new tool for automated image analysis (Wei, *et al.*, 2005) .

In the context of forestry applications using satellite images, the sensor measures the reflectance from the canopy surface which consists of individual tree in case of high resolution images. Thus most of the studies related to forestry using high resolution satellite images are concentrated on different stand parameters like land-cover, species composition, crown width, tree height (Mora, *et al.*, 2010), stand density and volume (Hirata, 2008) and isolation of individual tree crowns (Blaschke, *et al.*, 2004; Culvenor, 2002; Gougeon & Leckie, 2006) and canopy models are derived from this information.

The studies on tree parameters are based on the reflectance of the tree crowns. Estimation of Crown Projection Area (CPA) from their tree size *i.e.* Diameter at Breast Height (DBH) is very important both in Forest ecology, silviculture and Forest management (Shimano, 1997). Crown projection area is the portion that can be recognized in the image while DBH needs field measurement. Shimano, (1997) established a relationship between CPA and DBH. Similarly, a potential crown area is calculated from tree DBH by establishing a relationship between crown width and DBH (Pretzsch, 2009). Similarly, Cole & Lorimer (1994) found that basal area which is best estimator of DBH is the single best independent variable for predicting crown projection area of the exposed portion of the individual tree crown. Hirata, *et al.*,(2009) demonstrated significant relationship between DBH measured from the field and crown area derived from Quick bird panchromatic data. Song, *et al.*,(2010) established a significant statistical relationship between crown width and DBH and proved the potentiality of high resolution optical images to extract tree crown diameter in hardwood tree species as well. Even though there are few studies on crown width and DBH estimation of ABG and carbon stock are lacking. Anderson, *et al.*, (2000) developed regression models relating DBH and crown area and attempted to link the equations to geographic information system (GIS) but use of remote sensing to extract the crown features and estimation of carbon stock is a lacking. Thus, tree crown diameter which is found to be closely related to DBH (Hemery, *et al.*, 2005) can further be used to study forest biomass (Alves & Santos, 2002) and carbon stock. In addition, CPA was found to be the best independent variable for predicting basal area (Cole & Lorimer, 1994) from which biomass can be estimated.

Isolation of individual tree crowns provides improved species classification, and model tree structural parameters (Pouliot, *et al.*, 2002) useful not only in estimation of the carbon stocks and supporting the REDD programme but also in sustainable management of the forest.

1.5. Rationale and problem description

The tropical forest holds importance in ecosystem, but detailed ground-based quantifications of total carbon stocks are few (Sierra, *et al.*, 2007). Estimating AGB is still a challenging task, especially for the tropical and sub-tropical area which has complicated biophysical environments (Lu, 2005). Lack of information about global biomass due to uncertainties in accuracy and cost is still remaining as a matter of further exploration (Nguyen, 2010). In the context, Lu, (2006) highlights the essence of integrating field measurements with high resolution data and development of suitable procedure for AGB estimation. Zians & Mencuccini, (2004) also emphasize on need of rapid and easily implemented methods to assess

above ground woody biomass for carbon estimation which can be used to track changes in carbon stocks (Ketterings, *et al.*, 2001).

Diameter at breast height (DBH) and crown width are important tree characteristics (Bragg, 2001) to estimate the above ground carbon stock. But crowns of trees have been less subjected to mensurational study than their stems, primarily due to their lower marketable value, while, it has been very relevant in studies of the growth of stands due to the close correlation between crown size and stem diameter (Hemery, *et al.*, 2005). Only a few researches have been carried out on the relationship between crown widths and stem dimensions (Hemery, *et al.*, 2005; Hirata, *et al.*, 2009; Ozdemir, 2008; Song, *et al.*, 2010). Hemery, *et al.*, (2005) and Song, *et al.*, (2010) have demonstrated an allometric relationship between Crown diameter and DBH which adds to the potentiality of tree crown to infer other structural parameters using high resolution satellite imageries. However, tree crown size data are extremely scarce because they are very laborious to obtain in the field (Song, 2007). Gonzalez, *et al.*, (2010) expressed the need of study to accurately monitor the forest carbon from individual tree crowns obtained from high resolution satellites images. Asner, *et al.*, (2002) emphasized in developing more accurate model for estimation of crown dimensions using high spatial resolution satellite imagery. Though high-resolution satellites can detect individual tree crowns but the accurate monitoring of forest carbon has not been fully demonstrated (Gonzalez, *et al.*, 2010), automated techniques for grouping these into meaningful descriptions is still a challenge (Bunting, *et al.*, 2010). Apart from this the manual delineation cannot used in large areas as it is laborious to obtain. Using high resolution satellite images also reduces the cost of intensive sampling and its ability to estimate forest and tree parameters is high, but to do so, it is equally important to identify individual tree and crown area (Wang, *et al.*, 2004).

The high resolution images not only provide opportunity to isolate individual tree but also to differentiate the species as well (Ke, *et al.*, 2010). Though there have been studies of segmentation of individual tree crowns, the studies are limited when it comes to classification of species (Erikson, 2004). Among the few studies done of species classification, the accuracies obtained in classification is greater while using hyper-spectral data, as higher spectral resolution images has allowed more subtle differences (*e.g.*, in the red edge) (Bunting, *et al.*, 2010). This opportunity is provided by Worldview image with high spatial and spectral resolution.

Apart from aforementioned, national governments who have signed the UNFCCC and the Kyoto Protocol are bound by these agreements to report on the results of periodic national inventories of GHG emissions and removals, and forest carbon inventories (Andersson, *et al.*, 2009). Thus, Nepal being a signatory of UNFCCC has to estimate its carbon stock at national level. Besides, Community Forestry in Nepal is a global innovation in forest management (Ojha, *et al.*, 2009). It is an example to the world for its participatory approach, thus, this research aims to develop a method to estimate the amount of carbon in different CFUGs.

Thus this research aims to explore possibilities to derive carbon directly from tree crown area estimated from an image and establish a method for carbon accounting that could be used for similar forest areas in different parts of the world. In addition, ability of Geo-Eye and Worldview-2 in mapping carbon has not been considered widely in studies.

1.6. Objectives

The main objective of this research is to develop a method to accurately estimate carbon stocks in the sub-tropical forest using high resolution satellite images and object based image analysis.

The specific objectives

1. To assess the effect of image spectral characteristics for species classification using high resolution images and applying OBIA
2. To determine the relationship between Crown Projection Area (CPA) and carbon.
3. To estimate and map the amount of above ground carbon stock (as carbon stock hereafter) in the study area.

Research Questions

1. What is the difference in segmentation using GeoEye and Worldview images
2. What is the difference in classification using different spectral resolution images?
3. What is the relationship between CPA and Carbon?
4. What is the amount of carbon stock in the study area?

Hypothesis

- There is difference in segmentation accuracy between GeoEye and Worldview images
- Spectral characteristics improves the classification accuracy in species level
- There is a significant relationship between CPA and Carbon.

These objectives and research questions have been summarized in Table 1 with their respective research hypothesis.

Table 1: Research Objective, research questions and hypothesis

Objective	Research Questions	Hypothesis
1. To assess the effect of image spectral characteristics for species classification using high resolution images and applying OBIA	1. What is the difference in segmentation using GeoEye and Worldview images	H1: There is difference in segmentation accuracy between GeoEye and Worldview images.
	2. What is the difference in classification using different spectral resolution images?	H1: Spectral characteristics improves the classification accuracy in species level
2. To determine the relationship between Crown Projection Area (CPA) Carbon	3. What is the relationship between CPA and Carbon?	H1: There is a significant relationship between CPA and Carbon.
3. To estimate and map the amount of carbon stock in the study area	4. What is the amount of carbon stock in the study area?	

1.7. Theoretical Framework of research

The research started with literature review and identification of problem. The identified problem was used to formulate research questions. Data requirements were identified and fieldwork was carried out. The data collected were analysed. The results thus obtained are discussed and conclusion was derived. This process is shown in Figure 1.

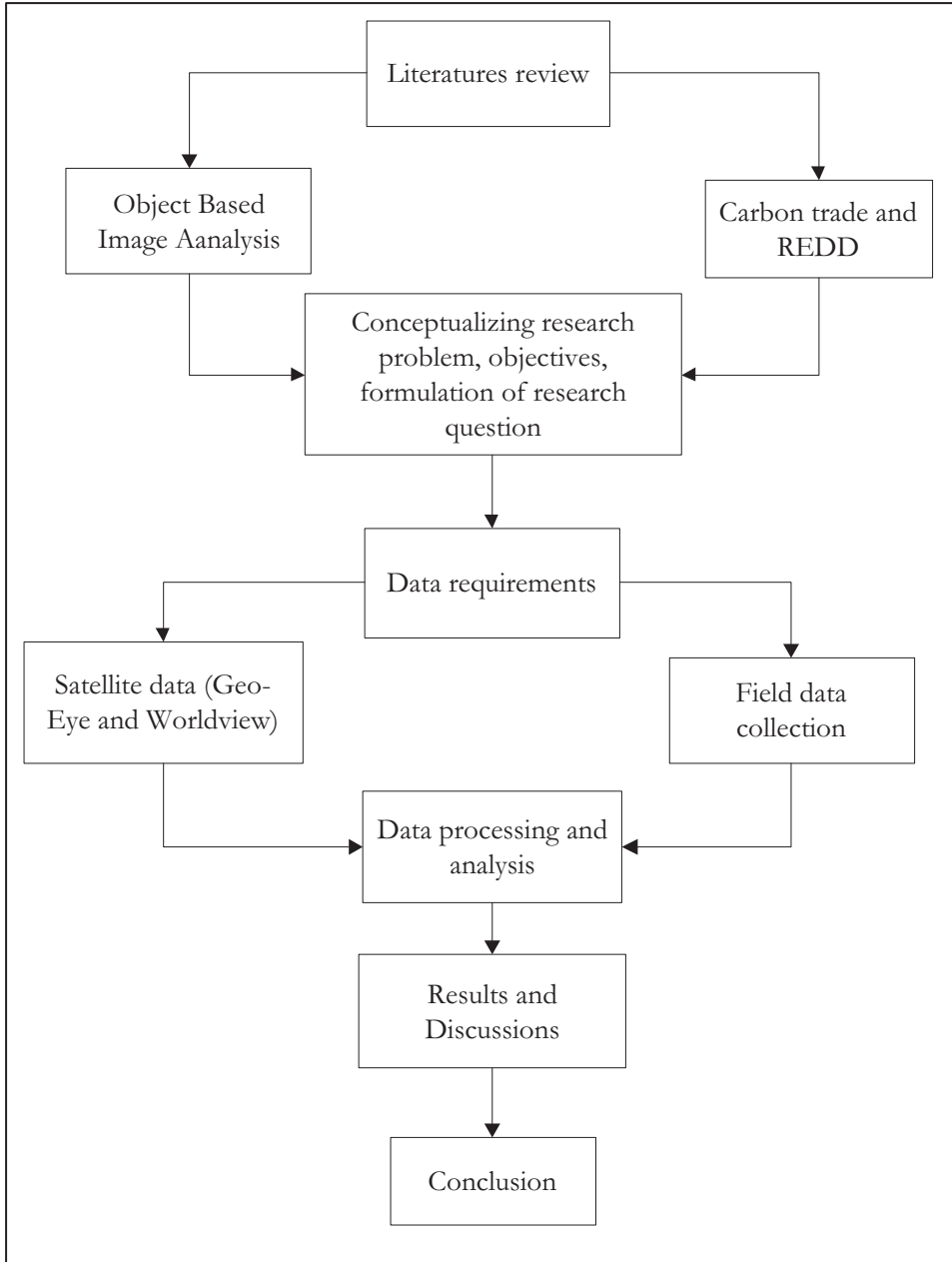


Figure 1: Theoretical framework of research

1.8. Concepts and definitions

1.8.1. Biomass and Carbon

Biomass refers to the dry weight of the trees. It includes the above ground biomass and below ground biomass (Figure 2), both living and dead, including soil organic matter, dead wood and litter (IPCC, 2007b). Above ground biomass is the biomass of all parts of tree above the soil and below ground biomass is the biomass of live roots more than 2mm diameter. But the carbon stored in AGB is the largest pool and most directly affected by deforestation and forest degradation (Gibbs, *et al.*, 2007). Dry woody biomass consists of forest carbon content which is obtained by multiplying the dry weight of a forest by 0.47. Thus, measurement of forest biomass can be used to estimate the carbon content of forests.

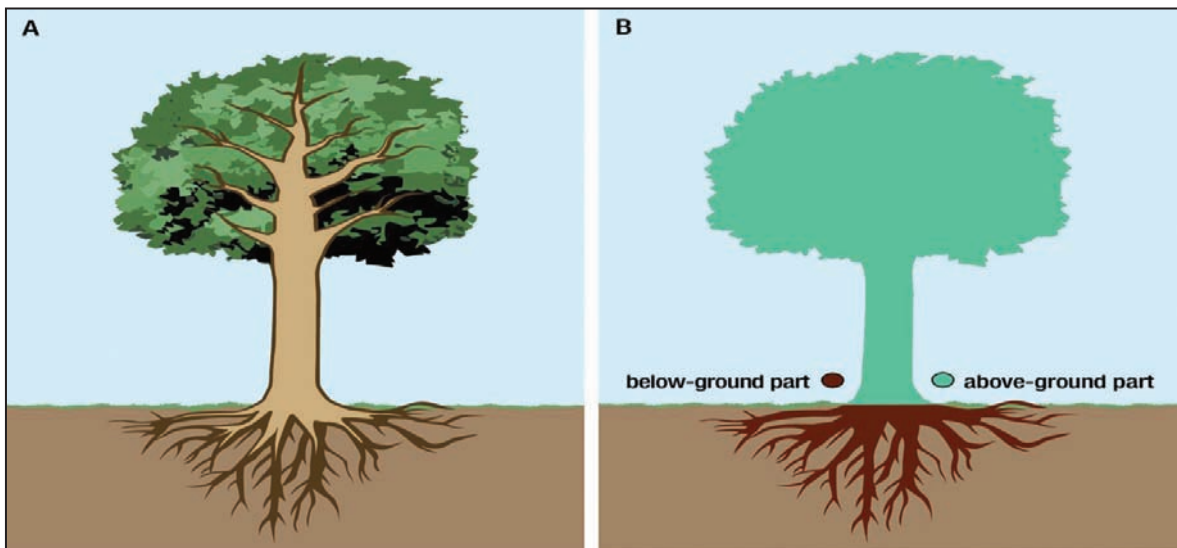


Figure 2: Biomass of a tree, Source: (Gschwantner, *et al.*, 2009)

1.8.2. Crown Projection Area

Crown area or crown projection area is defined as the proportion of the forest floor that is covered by the vertical projection of the tree crowns (Jennings, *et al.*, 1999) as shown in Figure 3. CPA is calculated from the maximum crown diameter assuming a circular crown projection (Kuuluvainen, 1991).

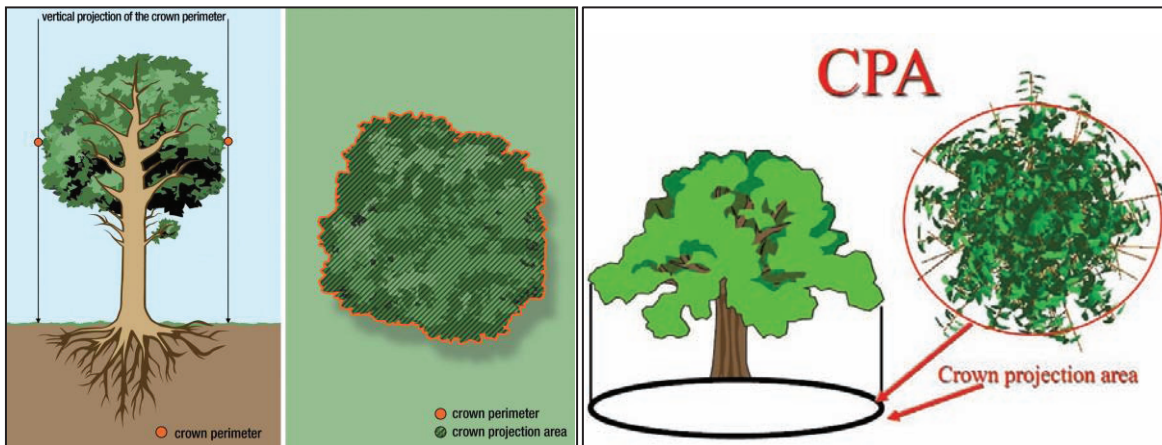


Figure 3: Crown Projection Area, Source: (Gschwantner, *et al.*, 2009)

1.8.3. Allometric Equation

Allometric equations are the quantitative relationships between measurable tree variables like DBH and height to other difficult to assess variables like standing volume of the tree or total biomass or carbon stock (Ketterings, *et al.*, 2001). For highly diverse tropical forests, Brown (2002) shows that reliable carbon estimates may be derived by using only DBH measurements and allometric relationships for broad categories of forest types and ecological zones.

1.8.4. Object Based Image Classification

The Object based image analysis also called as object oriented classification (Benz, *et al.*, 2004; Lillesand, *et al.*, 2008; Tan, *et al.*, 2010; Wei, *et al.*, 2005). Object-based approach refers to image processing techniques when applied result in the partitioning of an image into discrete non-overlapping units called image objects (Hay, *et al.*, 2005; Zhang, *et al.*, 2010). Being a part of the same object, an image-object is composed of spatially clustered pixels that exhibit high spectral relation (Hay, *et al.*, 2003). They are the basic entities which are composed of similarity not only in terms of spatial and spectral but also textural properties.

OBIA consists of two steps in classification. First step is to segment the image *i.e.* portioning of image in to contiguous, homogenous groups of pixels so as to form image objects. Second step is to classify these image objects based on spectral, textural, shape and contextual information (Cardoso & Corte-Real, 2005; Castilla & Hay, 2008; Zhang & Maxwell., 2006).

1.8.5. Community Forest

Community Forest is defined as the nationally owned forest handed over to a group of local people called as Community Forest User Groups (CFUGS) residing near the forest for development, conservation, and utilization of the resources. Through the government gives user groups rights of access, use, exclusion, and management but retains ownership of the land so that community forest lands cannot be sold or transferred (Thoms, 2008). The CFUGs is an autonomous body which plays a vital role in decision making and carry out the activities based on the constitution and operational plan. The forest technician is responsible to support in making constitution and operational plan of the CFUG.

2. STUDY AREA

2.1. Criteria for study area selection

The study area was selected using following criteria in mind.

- **Implementation of REDD programme**

Implementation of REDD pilot programme was considered as an important criteria for study area selection as carbon stock estimation holds significance to REDD mechanism.

- **Accessible and availability of data**

The study area selection was done taking accessibility into consideration because the study was to be done on limited time and budget. Since the Geo-eye image and other topographic maps were available Kayerkhola watershed was taken as study site for the research.

2.2. Overview of Chitwan district

Chitwan district lies in the central lowlands of Nepal. It lies at the distance of 150 km from Kathmandu, the capital city. It is located between 27°40'07"-27°46'37" northern latitude and 84°33'25"-84°41'48" eastern longitude. It is boarded by Dhading, Gorkha and Tanahun Districts in north while Parsa and India boarder the district from south. Makwanpur lies east to Chitwan and Nawalparasi borders in west.

2.2.1. Land use

The district has a huge amount of area under forest as it has two conservation areas in it. The world heritage site, Chitwan National Park covers an area of 970 km² and part of Parsa Wildlife reserve also falls in this district. Forest covers about 60% of the total land with area of 128500 ha. Similarly agricultural land and urban area account to 40% covering 89500 ha. The major land cover in Kayerkhola watershed is covered with forest which accounts for 5195 ha, barren land is 3.8 ha, bush area 264.4 ha, cultivation in 2268.6 ha and grassland covers 33.3 ha.

2.2.2. Social, economic and demographic

The watershed consists of social and ethnic diversity of the forest dependent indigenous communities. Chepang and Tamang are the dominant ethnic groups in the study area. These ethnic groups are one of the most marginalized ethnic groups in the country which makes them to highly depend upon forest resources for their livelihood. These communities also practice shifting cultivation, a traditional rotational agriculture system, which believed to be deteriorating the status of forest.

2.2.3. Climate

The average temperatures of the study area are 29^o-32^o maximum and 16^o-19^o minimum. The average rainfall in the study area is 1510 mm per year (Panta, 2003). July is the onset of monsoon thus the study area receives summer rain and winters are relatively dry.

2.2.4. Vegetation

Shorea robusta is the dominant species in the study area with *Lagerstroemia parviflora*, *Mallatus philippinensi* and *Terminelia tomentosa* as associate species.

2.2.5. Kayerkhola watershed area

It has 15 CFUGs and out of which only 5 CFUGs namely Kankali CFUG, Kalika CFUG, Dharampani CFUG, Devidhunga CFUG and Satkanya CFUG were taken for study due to limitation of the software to handle the big datasets and time availability for research. The study area has been shown in Figure 4. In all the CFUGs *Shorea robusta* forest is the dominant forest type which belongs to broader category of tropical broadleaved forest.

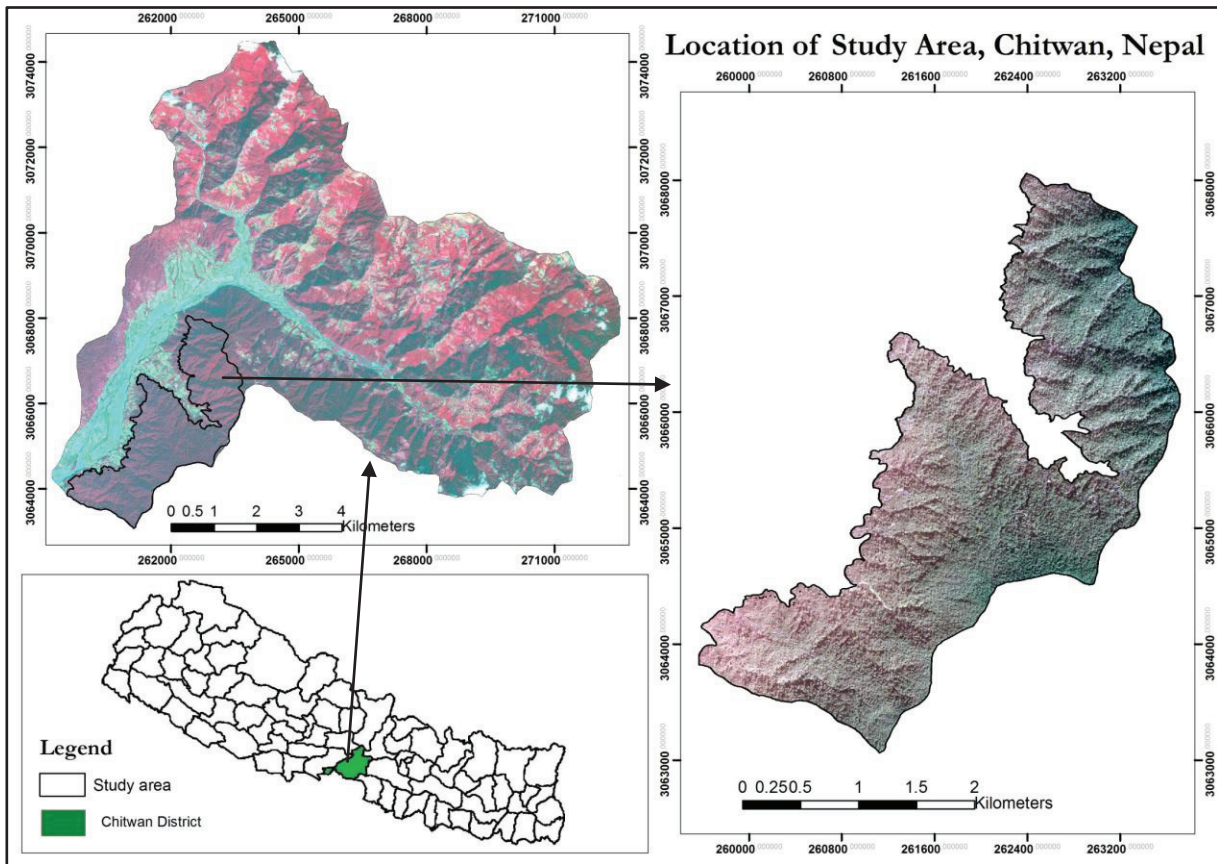


Figure 4: Location of study area, Chitwan, Nepal

3. MATERIALS AND METHODS

3.1. Data used

3.1.1. Satellite data

Two different satellite data of Kayerkhola watershed were used in the study. The Geo-eye image was obtained on 2nd November 2009. Geo-Eye multispectral image consisted of 4 bands in the visible part of the electromagnetic spectrum viz. blue (450-510 nm), green (510-580 nm), red (655-690 nm) and near infrared (IR) (780-920 nm) (GeoEye, 2010). The image at time of acquisition has 1.65m spatial resolution but it is distributed to customers only after resampling it to 2m resolution. Similarly pan image of Geo-Eye was also obtained from the same date which was originally 41 cm and was obtained after being resampled to 50 cm. The image obtained for the study was ortho-rectified and geo-referenced to the UTM WGS 84 coordinate system.

Worldview images obtained on 25th October 2010 is the first high resolution satellite image with 8 multispectral bands. Multispectral image has resolution of 1.84 cm resample to 2m and panchromatic of 46 cm resample to 50 cm. The bands include coastal blue (400-450nm), blue (450-510 nm), green (510-580 nm), yellow (585-625 nm), red (630-690 nm), red-edge (705-745), NIR₁ (770-895 nm) and NIR₂ (860-1040 nm) (DigitalGlobe, 2009). The Worldview-2 image was projected to Geographic (Lat/Lon) WGS 84 which was later re-projected to UTM zone 45N coordinates with WGS 84 datum. The image was ortho-rectified before obtaining for the study. The details of satellite data used are given in Appendix-1.

3.1.2. Maps

The maps used in this research are the topographic maps of the study area at scale of 1:25000 published by Survey Department of Government of Nepal in 1994. The watershed boundary, Community forest shape files of study area were obtained from ICIMOD, 2009.

3.1.3. Software

Different software as shown in Table 2 were used to facilitate the research. The image analysis was done using Erdas imagine 2010 and eCognition Developer 8 software was used for object based image analysis. ArcGIS was used to carry out GIS operations. Microsoft Office and other statistical packages were also used in the study.

Table 2: Software used in the research

S.N	Software	Purpose
1	ArcGIS version 10	GIS analysis
2	eCognition Developer 8	Object based image analysis
3	Erdas Imagine 2010	Image processing and remote sensing applications
4	SPSS	Statistical analysis
5	Microsoft Excel	Statistical analysis
6	XL-stat	Statistical analysis
7	Microsoft PowerPoint	Presentation of research
8	Microsoft Visio	Diagrammatic representations
9	Microsoft Word	Writing thesis

3.1.4. Filed equipment

Various equipment as shown in Table 3 were used during the fieldwork. GPS, iPAQ were used for navigation to the plot and recording the centre of sample plot. Diameter of the tree was measured using diameter tape; height of the tree was measured using haga altimeter. Field dataset was used for field data collection (Appendix-2).

Table 3: Field equipment used for the study

S.N	Equipment	Purpose
1.	Garmin GPS and iPAQ	Navigation
2.	Diameter tape (5m)	Diameter measurement
3.	Measuring tape (30m)	Measuring the radius of plot
4.	Haga altimeter	Height measurement
5.	Field work dataset	Field data collection

3.2. Image pre-processing

Image pre-processing is also called as image restoration and rectification which requires further manipulation and analysis of the image data to extract information (Lillesand, *et al.*, 2008). It is done to correct the sensor and platform-specific radiometric and geometric distortion of the raw data and aims to correct the distorted or degradation of the image generated at the time of acquisition. There are various sources of image distortions namely geometric distortions and radiometric corrections. The images obtained were ortho-rectified hence ortho-rectification was not done.

3.2.1. Image mosaic and subset

The worldview-2 image was obtained in two separate images so the first operation done was to mosaic the image before projecting it to UTM WGS 84 coordinate system. This task was performed in ERDAS 2010. The image was also subset to extract the study area from the whole image. Sub-setting of the image was required for both the images.

3.2.2. Image fusion

“Image fusion refers to the acquisition, processing and synergistic combination of information provided by various sensors or by the same sensor in many measuring contexts” (Simone, *et al.*, 2002). It is the process of merging two or more images in such a way as to retain the most desirable characteristics of each. When a panchromatic (PAN), image is fused with multispectral imagery, the desired result is an image with the spatial resolution and quality of the panchromatic imagery and the spectral resolution and quality of the multispectral imagery (Amolins, *et al.*, 2007). Thus, pan-sharpening is a technique that fuses the information of a low resolution multispectral image and a high resolution PAN image, to provide a high resolution multispectral image (Amro & Mateos, 2010)

Geo-Eye multispectral image of 2 m resolution was fused with Geo-Eye panchromatic image of spatial resolution 50 cm and a pan-sharpened image with spatial resolution of 50 cm was obtained. Different fusion techniques like Intensity Hue Saturation (IHS) and high pass filter (HPF) resolution merge were tried to obtain better image for analysis. IHS gave better visual appearance while HPF was spectrally appealing.

IHS processes only three bands at a time. This pan-sharpening process follows three distinct steps. First a multispectral band is transformed from RGB to IHS space. Secondly, intensity of low resolution multispectral image is replaced by intensity of high spatial resolution image, then the original hue and saturation and new intensity images are transformed back to RGB display for visualization.

In case of HPF resolution merge, small high-pass filter is applied in PAN image, then this result is combined with the lower resolution multispectral data on pixel to pixel (Chavez, *et al.*, 1991), resulting in higher spatial as well as spectral resolution data set. The advantage of using HPF is to maintain the spectral properties of the original multispectral image. It results in all the bands of original multispectral image with spectral resolution of pan image.

3.2.3. Image filtering/Convolution

Image filtering is an image enhancement technique which improves the visual interpretability of an image by increasing the distinction between the scenes. A moving window/ kernel which contains an array of coefficient or weighing factors is established and moved over the original image. The output is obtained by multiplying each coefficient in the kernel by the corresponding digital number (DN) in the original image and adding all the resulting products (Lillesand, *et al.*, 2008). The low pass filter was used to smoothen the appearance of the image. The low pass filter was applied in the images for manual delineation of the crowns and also in segmentation of the images.

3.3. Research Method

The research method followed three distinct step *i.e.* Remote sensing, Field work and statistical analysis. The organization of these steps is shown in Figure 5: Methods Flow Chart. Field work was carried out to obtain DBH and other measure while remote sensing operations were needed to obtain individual tree crown. The statistical analysis was done to obtain the relationship between DBH and crown area to map the carbon stock.

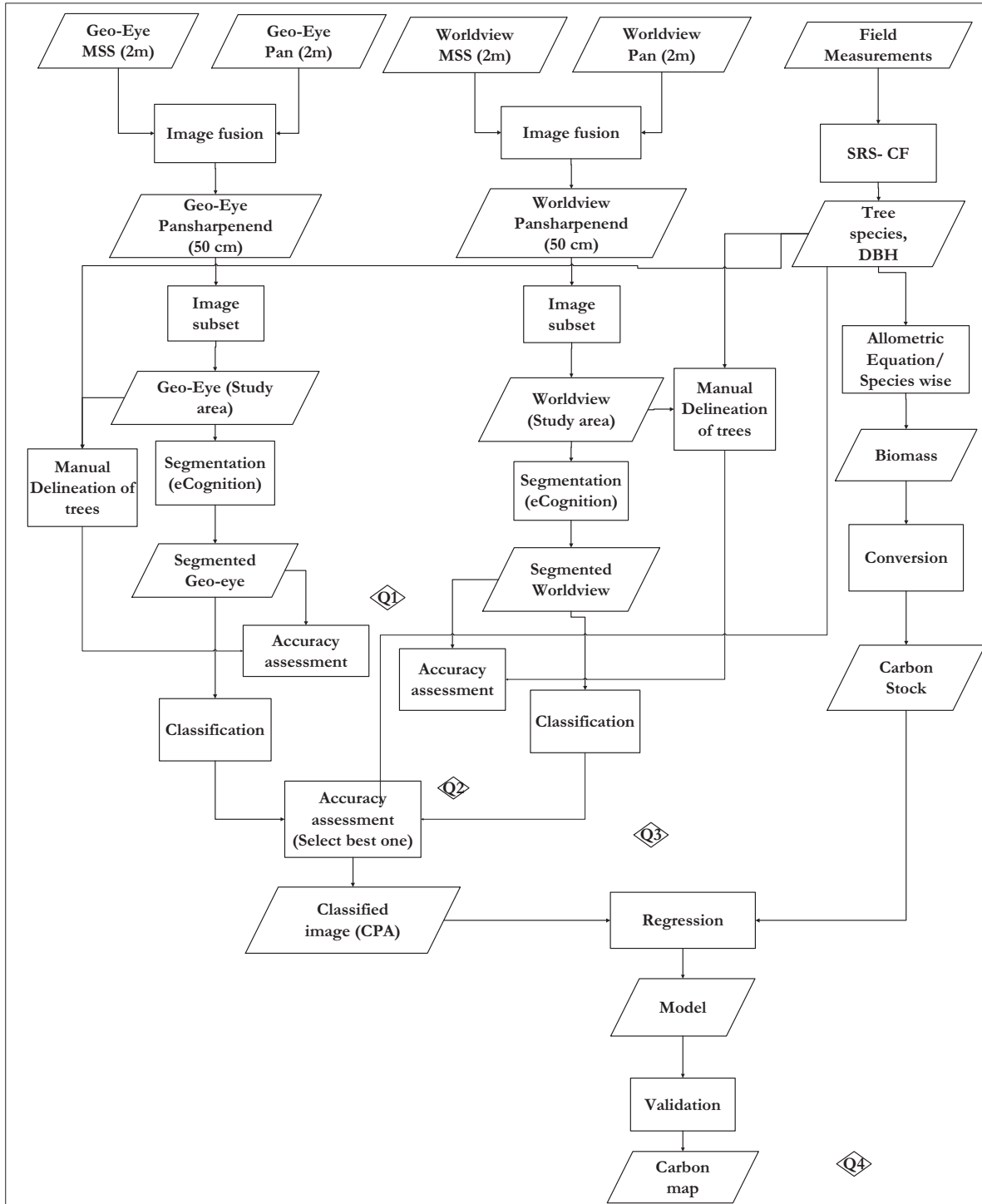


Figure 5: Methods Flow Chart

3.4. Field work

3.4.1. Sampling design

Sampling design was done before the fieldwork for selecting the sampling plots. As stratification often yields more precise estimate of the forest parameters than done by random sampling of the same size (Husch, *et al.*, 2003), the study area is divided into 15 broad strata based on number of community forests. In each stratum random sampling was done. A large number of plots allow the estimation of spatial variability of carbon stocks, which increases the confidence in the Carbon estimates. Thus, to ensure enough number of sample plots, following formula was used.

$$n = \frac{t^2 * CV^2}{AE^2} \dots\dots\dots \text{Equation 1: Sample size}$$

Where, n= minimum number of samples required
 t= t value associated with specified probability
 CV = Coefficient of variance
 AE= Allowable error (Husch, *et al.*, 2003)

The number of samples each stratum was in proportion to the area of the strata. But there is also disadvantage of using stratified random sampling as the size of each stratum should be known beforehand (Husch, *et al.*, 2003). Land use map of the study area was used to facilitate in spreading the samples in the study area. Sample map (Appendix-1) was prepared before the fieldwork so that the trees could be easily recognized. Other necessary preparation like collection of field instrument, data collection format development, and image uploading in iPAQ was also done before departing for the fieldwork.

3.4.2. Data collection from field work

Field work was carried out in September- October 2010. Field work is required to measure DBH as it is the predictor of carbon estimation. DBH is measured from the study area which will help as ground truth data for estimation of the biomass as well as validation of the model. Circular plots of radius 12.62 m with plot area 500m² (Husch, *et al.*, 2003) were established in the field with the help of iPAQ and global positioning systems (GPS Map 60CSx, Garmin). GPS was used to navigate to the plot centre. Measurement of DBH alone or in combination of height can be converted to estimate carbon stock using allometric equation (Gibbs, *et al.*, 2007). So, with the assigned radius the trees with diameter more than 10 cm were measured at breast height *i.e.* 1.30 m from the ground level. It is generally assumed that the trees with diameter 10 cm or less contribute little to the total biomass carbon of a forest and thus they are often not measured (Brown, 2002). Other topographical features like slope and aspect were taken into consideration. For the areas with slope greater than 5%, slope correction was applied.

3.4.3. Sampling Plots

Tree parameters were measured in 63 plots according to the original study area which covered the whole Kayerkhola watershed but due to limitation of the eCognition software to handle the large dataset, the study area was limited to 5 CFUGs instead of 15 CFUGs. Hence samples from 19 plots collected by the researcher are used while samples in 12 plots were collected by ICIMOD (INGO) staff in June. The location of sample plots is given in Appendix-3.

3.5. Field work data analysis

After field work, all the data collected in the field were entered in appropriate format and descriptive analysis was done as shown in Appendix-4. The trees that were recognized in image during the fieldwork were delineated using ArcGIS. These delineated tree crown area was used for validation of segmentation accuracy as well for validation of the regression model.

3.5.1. Manual delineation of trees

Manual delineation of the identified trees was done after the fieldwork for validation of the model as well as validation segmentation accuracy. Manual delineation was done on 5*5 filtered image so that the trees would be smooth. Delineation of the individual trees was done based on certain rules *i.e.*

- Use of same scale for delineation *i.e.* scale for delineation was 1:250.
- Use of crown width as reference for delineation of the trees
- Done only of the trees that were actually recognized in the field

Geo-Eye and Worldview crowns were separately delineated. Though 149 trees were recognized in the field only 130 trees could be delineated in the image in Geo-Eye image, while only 90 trees could be recognized and delineated in Worldview image.

3.6. Segmentation of images

Segmentation is a spatial clustering technique, which leads an image to subdivide into non-overlapping units or segments (Möller, *et al.*, 2007). It is a building block of object based image analysis, hence, the determination of segments is very important (Kim, *et al.*, 2008) in identifying homogenous areas and group them into specific objects. There are various types of segmentation techniques available, the major ones being edge based and region based segmentation techniques. In this study region based technique is used.

Region based segmentation algorithms extract information from the image by grouping spatially and spectrally similar pixels into homogenous area to form an image object. This segmentation approach is called bottom up segmentation algorithm which refers to assembling objects to create a larger objects (Definiens, 2009b). Region-based segmentation thus can be divided into three techniques viz, region growing, region merging and region splitting.

Region-growing algorithm starts from single pixel or from a seed pixel which subsequently merges and grows until a certain threshold reached *i.e.* the pixels are merged and grown until no more pixels can be merged or grown, then new seeds are placed and process is repeated (Blaschke, *et al.*, 2004). The smaller image objects are merged with the bigger ones and the merging is based homogeneity criteria. Homogeneity criteria is based on colour, smoothness and compactness parameters which determines the within- segment heterogeneity (Carleer, *et al.*, 2005).

Region-merging algorithm merge segments starting from the initial regions which may be single pixel of object determined and in region-splitting algorithm large segments are divided into smaller units based on the homogeneity criterion. In this study multi-resolution segmentation a region-based segmentation approach was used.

3.6.1. Multi-resolution segmentation

Multi-resolution segmentation is a region based algorithm for image segmentation (Rejaur & Saha, 2008). For a given number of image objects, it minimizes the average heterogeneity and maximizes their

respective homogeneity so as to produce meaningful objects. The procedure for multi resolution segmentation is outlined below.

- The segmentation starts from a single pixel regarded as seed from one image object and it repeatedly merges the pixels in series of loops until the homogeneity is reached. The homogeneity criterion for multi resolution segmentation is defined by scale and shape parameters.
- The seed looks for its best-fitting neighbour and assembles/merges the neighbour in it.
- If best fitting is not agreed or if it is not mutual then best candidate image object becomes the new seed image object and finds its best fitting partner.
- When best fitting is mutual, image objects are merged in each loop. The loops continue until no further merging is possible. The procedure then starts with another image object.

Multi-resolution segmentation was carried out in eCognition Developer 8 software.

3.6.2. Scale parameter

Scale plays an important role in determining the object size. It determines the occurrence and absence of an object (Benz, *et al.*, 2004). When scale parameter is altered the same object appears differently. When the purpose is to do land-cover classification scale used will be big while in identification of trees, the scale parameters should be small.

The Scale Parameter is a term that is used to determine the maximum allowed heterogeneity for the resulting image objects. If the data is heterogeneous then the resulting image objects for certain parameters will be smaller than in more homogeneous data. By modifying the value of scale parameter the size of the objects required can be accommodated. The homogeneity of the objects on which the scale parameter refers to is called composition of homogeneity which depends upon colour, smoothness and compactness. The value of shape field modifies the relationship between shape and colour criteria, (colour= 1-shape) so, decreasing the shape value will increase the colour criteria (Definiens, 2009a). The compactness criteria is used to when different image objects are rather compact and are separated from non-compact objects only by relatively weak spectral contrast. The relationship between these components of composition of homogeneity is shown in Figure 6. For this study scale parameter was set to 19 in Geo-Eye and 21 in Worldview image with shape 0.8 and compactness 0.5.

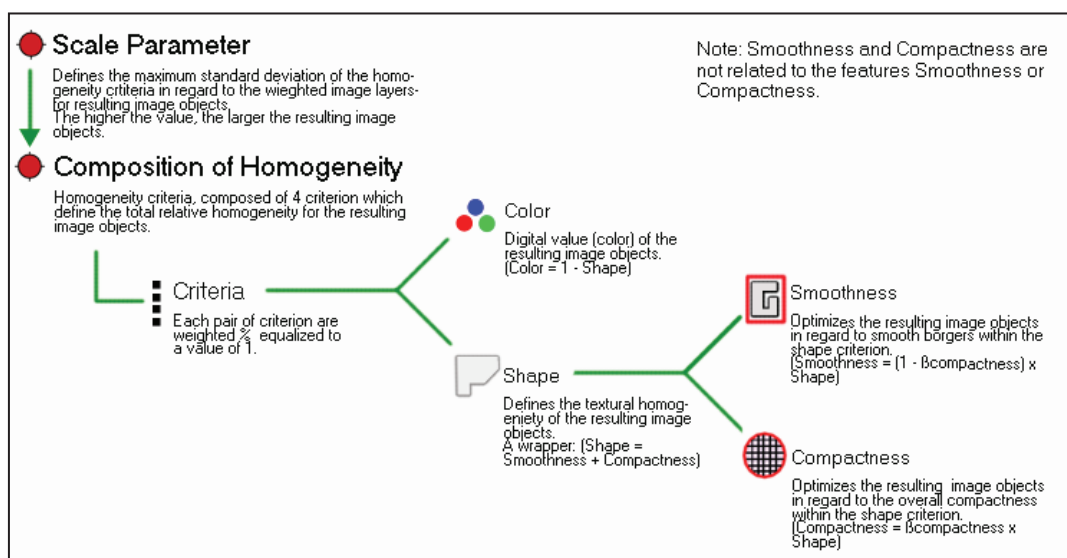


Figure 6: Multi-resolution segmentation concepts flow

Since multi-resolution segmentation is an iterative process, choice of scale parameters is very important as has a great influence on the segmentation results (Carleer, *et al.*, 2005). Hence ESP tool was used as a support in deciding the best fit scale parameters to be used in the segmentation procedure.

3.6.3. Estimation of Scale parameter

The ESP tool works in a bottom up approach as it iteratively generates image-objects at multiple scales. It calculates the local variances for each scale. The variation in heterogeneity is explored by plotting local variance against the corresponding scale (Drăguț, *et al.*, 2010). The thresholds in rates of change of local variance indicate the scale levels at which the image can be segmented in the most appropriate manner (Drăguț, *et al.*, 2010). Figure: 7 shows ESP tool used for determining the scale parameter.

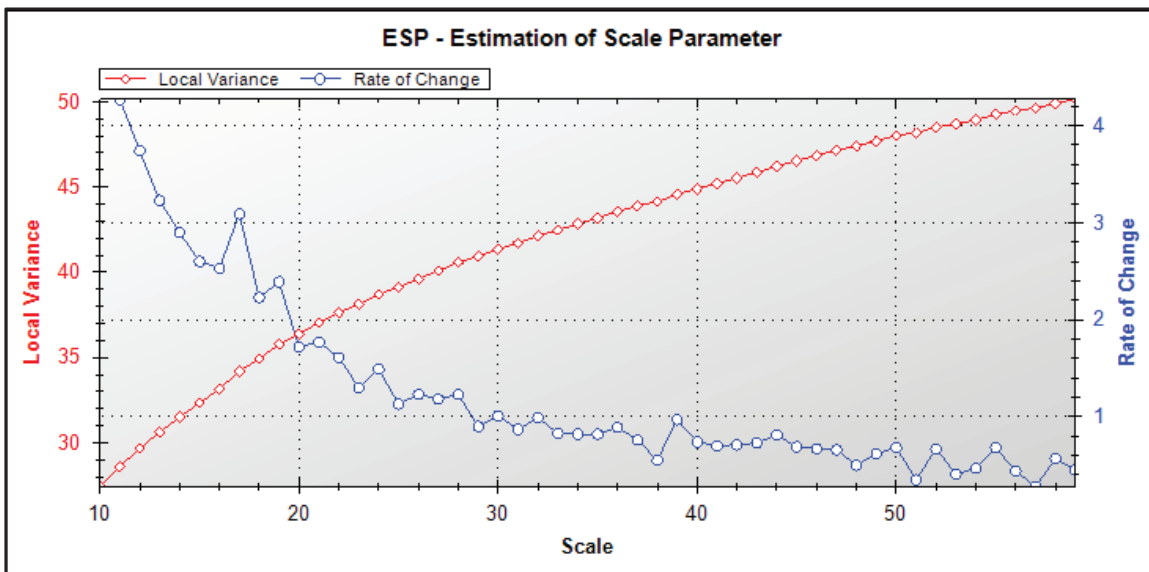


Figure 7: ESP tool for determining scale

3.7. Procedure of Segmentation

Segmentation in this study has been carried out in series of steps. Pre-processing of the image was followed by multi-resolution segmentation. Watershed segmentation and morphological operations were carried out to obtain an individual tree. This process has been illustrated in Figure: 8. the appearance of trees in 3D view is shown in Figure 9.

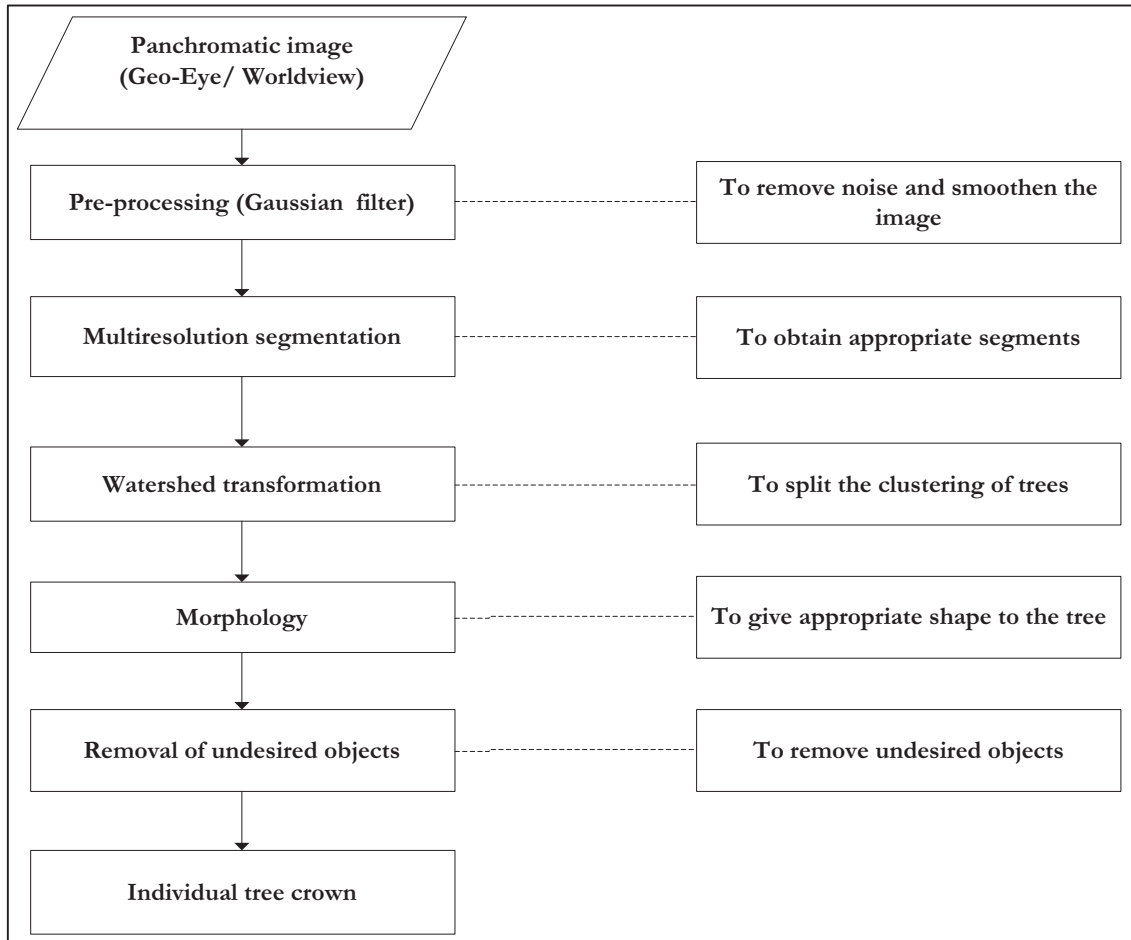


Figure 8: Segmentation process

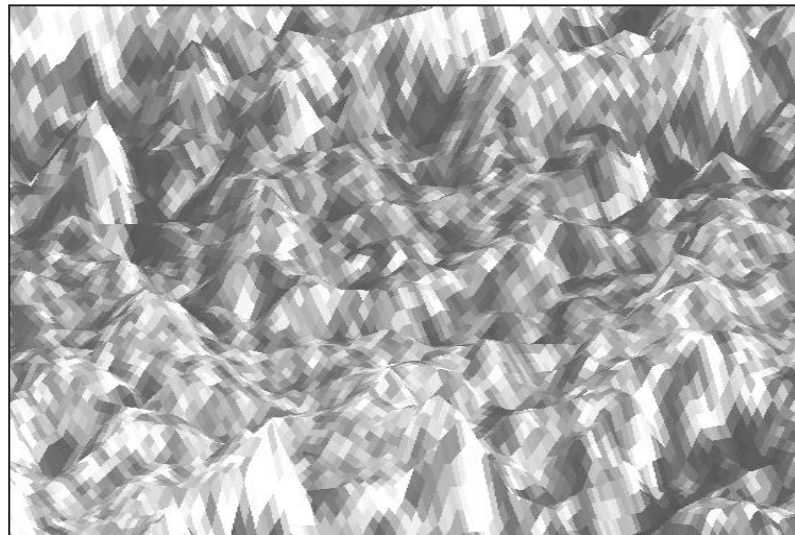


Figure 9: 3D view of the Geo-Eye image

3.7.1. Pre-processing in eCognition

The pre-processing for segmentation was done using eCognition. Convolution Gaussian filter was applied to the panchromatic image. This filter was chosen as it removes the noise and also intensity of variation due to trees internal structure $7*7$ kernel was used. The convolution filter uses a kernel which is a square matrix of a value that is applied to the image pixels and each pixel value is replaced by the average of the square area of the matrix centred on the pixel (Definiens, 2009a)

3.7.2. Masking out shadow and cloud

Because of high spatial resolution of the images used and viewing angle shadow was prominent in both Geo-Eye and Worldview images. So, first step to do before segmenting the image was to mask out the shadow and cloud. The values which were very high compared to rest of the pixel brightness values were regarded as cloud *e.g.* in Worldview image, the pixels with brightness value greater than 600 were masked out as cloud. Similarly the pixels which showed very low brightness value were masked out as shadow in both the images. The pixels with values less than 310 were masked out as shadow in case of Geo-Eye and the value was bit higher 320 in case of Worldview image.

3.7.3. Parameters Setting using ESP

Scale parameters for multi-resolution segmentation was done using ESP tool, though series of trial and error with different scales was also done. ESP tool was used to set the scale parameters in both the images. The rule-set developed for ESP tool was loaded in eCognition to get the optimum scale parameters for both the images.

3.7.4. Watershed transformation

After multi-resolution segmentation, watershed transformation was done. Watershed transformation was done to address the intermingling situation of the natural forest. This algorithm helps to split the overlapping tree crowns into individual tree crowns based on the splitting threshold. This threshold is given on the basis of expert knowledge on crown width.

Watershed transformation first calculates an inverted distance map. This map is calculated based on the inverted distance for each pixel to the image object boarder and this makes the maximum value in original image to become minimum value in the inverted distance map (Definiens, 2009a). The image looks like a watershed catchment. When water is introduced in the system then each valley will collect water from local minima until water spills to the adjacent valley (Wang, *et al.*, 2004). When the individual catchment basins touch each other the objects are split which helps to reduce the overlapping of crown. Thus, when applying watershed transformation to the forest, tree clumps are treated as the catchment and under flooding water assumption, the trees (as valleys) touch each other, and then the trees are separated into individual trees.

3.7.5. Morphology

Morphology operation was carried out to smooth the boarder of image. eCognition gives two basic operations in morphology *i.e.* close image objects and open image objects. Open image object removes the pixel which is isolated from an image object while close image objects will add surrounding isolated pixel to an image object. In this study, close image object operation was done so that the smaller holes due to shadow and difference in spectral properties will be filled. Morphology also provides an option to define the shape and size of the mask. The mask is a structuring element on which the morphology is based. Circular and square masks are available in eCognition. Circular mask was created as the trees crowns are circular in shape.

3.7.6. Removal of some undesired objects

After completing the segmentation procedure some very tiny object with object area less than 16 pixels were removed as they had crown diameter of less than 2m whose reflectance would be difficult to be detected in a dense forest. Similarly some elongated features in the segmented image were removed.

3.8. Segmentation validation

Segmentation of an image is incomplete without validation of the results. Segmentation validation is related to quality of data (noise, spatial and spectral resolution) and the optimal customization of parameter settings (Möller *et al.*, 2007). Since image objects are extracted based on the thematic and geometric components of objects (Zhan, *et al.*, 2005) quality assessments have to be considered in terms of their topological and geometrical relationships (Möller *et al.*, 2007). Topological relationships of interests are ‘containment’ and ‘overlap’, whereas; geometric relationships can be determined by the comparison of object positions.

One of the methods to validate the segmentation is by using reference polygons from manual digitization to test the automatic segmentation (Benz, *et al.*, 2004; Möller, *et al.*, 2007). If the reference polygon is completely covered by automatically achieved segments, best scores are given (Benz, *et al.*, 2004).

Validation of the segmentation in this study was done by matching the manually delineated segments with the automatic segments and comparison was made in terms of area overlapped *i.e.* the topological and also in terms of position so both the topological and geometric relationships are considered. In a research done by Zhan, *et al.*, (2005) matching of reference object with extracted or segmented objects was done and it was considered to be matching if the reference and extracted objects overlap by at least 50%. One to one matching takes position, size and shape of an object into consideration apart from this, it also takes completeness and correctness into consideration (Zhan, *et al.*, 2005)

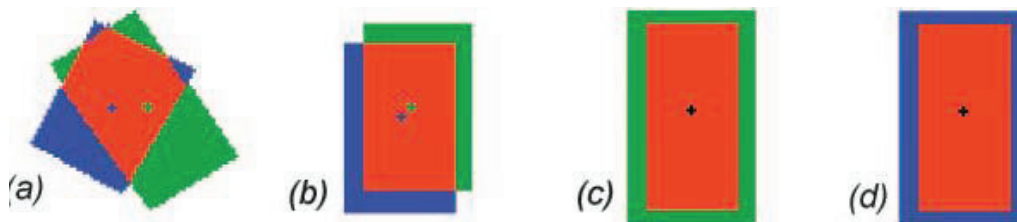


Figure 10: After (Zhan, *et al.*, 2005) showing different conditions of one to one matching

Figure 10, shows the matching conditions of different reference object with automatic segmented objects. The part that is in red is the matched region while green is the region that is not explained by the reference object. Case a) shows more than 50% match between reference and segmented object. b) Shows the same shape and size of the object match with each other but with difference in location c) and d) the reference and segmented objects match from positional context but differ in spatial extent.

3.9. Image classification and accuracy assessment

3.9.1. Transformed divergence (D_T)

Transformed divergence is the statistical distance between the pairs of signatures to maximize the separability. It is done to estimate the probability of correct classification between pair of classes. The class pairs with highest D_T maximize the likelihood of high classification accuracy. It has both the upper and lower bounds. The scale of the divergence values can range from 0-2000. If D_T is greater than 1900, then

the classes can be separated. When D_T is between 1700 -1900, the separation is fairly good and below 1700, the separation is poor (Jensen, 1986). If the calculated divergence is equal to upper bound then the signatures can be said to be totally separable in the bands being studied *i.e.* if the D_T 2000 meaning that the classes are totally separable. It is based on the covariance and the mean vectors of the signatures are compared to determine which set of the band is most useful for classification.

3.9.2. Image classification

Object based image classification is based on a fact that important semantic information needed to interpret an image is provided by an object and its mutual neighbourhood relations but not only in a single pixel. This method takes spectral, spatial and contextual information necessary to interpret an image. There are two different kinds of classification approaches in eCognition *i.e.* membership function and nearest neighbour.

Nearest Neighbour classification in eCognition is based on a fuzzy classification algorithm and classified image objects have a membership to more than one class. The smaller the difference is between sample objects and the object to be classified, the higher is the membership value (Laliberte, *et al.*, 2006). If there is greater degree of membership between the best and second best class assignment, the classification is better yielding better classification stability. Thus, supervised nearest neighbour classification of the image was done for the study. This algorithm uses samples of image objects from each class as training samples and classifies the image objects by comparing their feature property with the provided samples (Joshi, 2010).

Classification at species level was done and at least one species was be classified. The trees that were recognized and annotated in the field were taken for classification of the species. Classification was done on HPF image with maximum weight on infra-red bands.

3.9.3. Accuracy Assessment

Accuracy assessment is done in the number of raster elements of the output are selected and both the classification result and true world classes are compared (Kerle, *et al.*, 2004) and the comparison is done using error matrix which computes the overall accuracy of the classification. Accuracy assessment was done in Erdas Imagine 2010.

3.10. Above Ground Biomass and Carbon Stock calculation

The most common method for estimating forest biomass is through allometric equations (Ketterings, *et al.*, 2001) which can then be used to estimate carbon stock of forests (Basuki, *et al.*, 2009) using conversion factor which accounts to 0.47 (IPCC, 2006) tonnes of above ground biomass. So, species wise allometric equation is used to estimate the AGB of *Shorea robusta* while for other species IPCC general broadleaf equation of study area. Both of the equations use only DBH to estimate the biomass.

The allometric equations that is used for the study are

i. $\text{Ln (TAGB)} = -2.193 + 2.371 * \text{Ln (DBH)}$ Equation 2: Allometric equation for *Shorea robusta*

with 1.034 as correction factor (Basuki, *et al.*, 2009) for *Shorea robusta*. The equation was originally developed for East Kalimantan, Indonesia but since the average rainfall and mean annual temperatures of both the areas are similar, this equation is used.

Where, TAGB = Total above ground biomass,
 DBH= Diameter at breast height

ii. $Y = \text{EXP} [-2.289+2.649*\text{Ln}(\text{DBH})-0.021*(\text{Ln}(\text{DBH}))^2]$ Equation 3: Allometric equation for class "other"

IPCC for Tropical moist hardwoods will be used for other species. Tropical moist generally represent areas with rainfall of between 2000 to 4000 mm/year in the lowlands(IPCC, 2007a).

Where, TAGB = Total above ground biomass,
 DBH= Diameter at breast height

The total above ground obtained from these equations will be converted to carbon stock using a conversion factor (IPCC 2011).

$$C=B * CF$$

Where, C= carbon stock (MgC)

B= Dry biomass

CF= Carbon fraction of biomass (=0.47)

3.11. Regression Analysis and validation of the model

Regression analysis is done for determining the relationship between dependent and independent variable and works on the cause and effect relationship. The change in independent variable results in change in dependent variable (Husch, *et al.*, 2003). A non-linear relationship between carbon and CPA was established to develop a regression model for carbon estimation directly from CPA.

Those individual trees which were correctly classified and had one to one matching of the segments were used for model development and validation as falsely identified or misclassified trees cannot be used for evaluation (Pouliot, *et al.*, 2002). Apart from this few outliers were also removed which is the prerequisite of regression models to establish a robust model (Mora, *et al.*, 2010). Thus, the number of observations becomes less than the trees that were actually collected/ recognized in the field. Out of 130 recognized in the field, only 89 were used for the purpose.

The model thus obtained was validated using the test data set obtained from the field. Validation of the model was done by comparing the amount of carbon predicted by the model and amount calculated from the field data. Root mean square error (RMSE) is calculated to check the amount of error in the carbon stock map.

$$RMSE = \sqrt{\frac{\sum (Cp-Co)^2}{N}}$$
Equation 4: RMSE

Where, RMSE = Root Mean Square Error,

Cp- Carbon predicted by the model

Co-Carbon calculated.

N-Number of observations

4. RESULTS

4.1. Image segmentation

Image segmentation was done on panchromatic images of Geo-Eye and World view respectively. Multi-resolution segmentation was carried out to group the pixels into homogenous area to form an object. Shadow was masked out from the image for segmentation process so as to avoid overestimation of the crown projection area.

4.1.1. Estimation of Scale Parameter

Estimation of Scale Parameter (ESP) tool was used to find the most appropriate scale for multi-resolution segmentation. Figure 11a shows the estimation of scale parameter of Geo-Eye image, which shows that scale parameter 19 or 21 are the appropriate scales to segment the image. Similarly Figure 11b shows the scale parameter appropriate for Worldview-2 image, which shows scale parameter either 18 or 21 to be most appropriate.

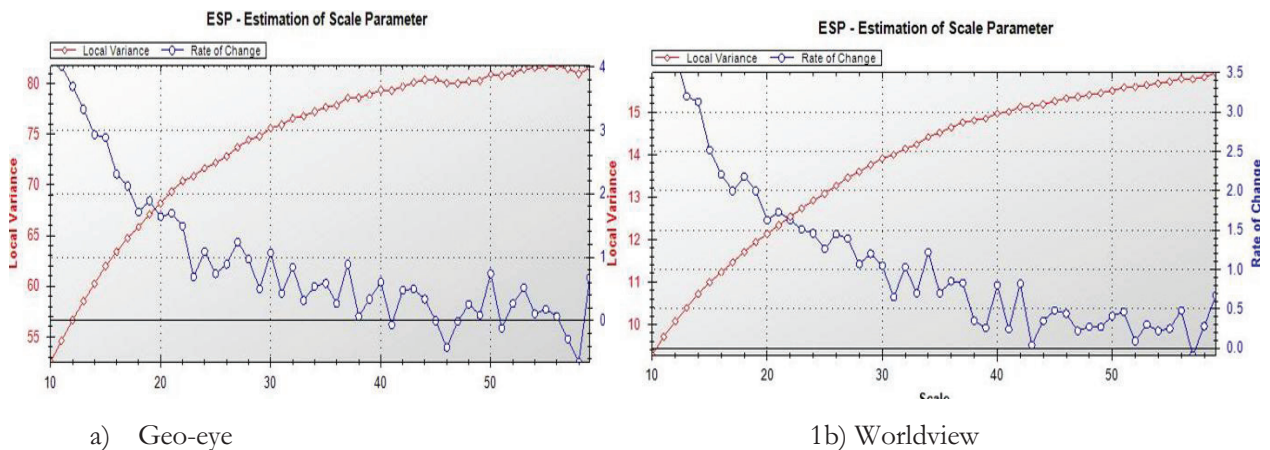


Figure 11: ESP tool of Geo-Eye and Worldview-2 images

4.1.2. Multi-resolution segmentation

In spite of using ESP tool to identify the best scale parameter, different scales *i.e.* 18, 19, 21 were used to find out the most appropriate scale to be used for further analysis. These scales are the peak values of rate of change determined by ESP tool in Figure 11. The “D”- value was calculated for these 3 peaks to obtain more accurate segmentation. “D”, a measure of “goodness of fit” is used to obtain the over-segmentation and under-segmentation ratio which helps to decide on the parameter to be used. The “D”-value ranges from 0-1 and value closer to 0 is the best value with the objects (reference and segmented) exactly overlapping each other meaning that there is no problem of over-segmentation and under-segmentation. Table 4 shows the “D-value” obtained for Geo-Eye and Worldview-2 images. Since the value 0.36 obtained by segmenting the Geo-Eye image with scale parameter 19 is the closest value to 0, scale parameter 19 was regarded as most appropriate to segment Geo-Eye image. Similarly, in case of Worldview image, scale parameter 21 was found to be most appropriate with its value closest to 0.

Table 4: "D" value of different segmentation scales as determined in Figure 11.

Scale	21	19	18
D-value-Geo-Eye	0.41	0.36	0.41
D-value-Worldview-2	0.40	0.47	0.45

Based on the above scale parameters as described in Table 4, multi-resolution segmentation was carried out in both Geo-Eye and Worldview-2 images. Figure 12 shows the final output of multi-resolution segmentation.

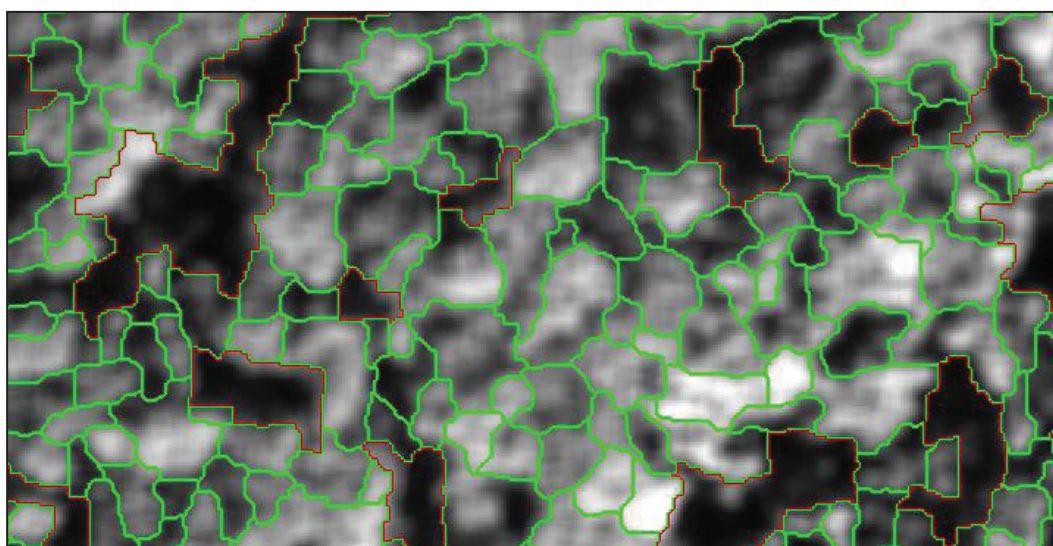


Figure 12: Multi-resolution segmentation of Geo-Eye image (Green colour lines showing trees and brown colour lines showing shadow region)

4.1.3. Segmentation accuracy

Segmentation accuracy was assessed by matching the objects on a one to one basis. Overall segmentation accuracy for Geo-eye was found to be 77.6%. Out of 130 reference polygons obtained from manual delineation, only 101 automatic polygons obtained from segmentation had one to one relationship. Whereas Worldview image accounted to 74.4% accuracy as 69 segmented polygons out of 90 reference polygons were correctly segmented. This result has been demonstrated in Table 5.

Table 5: Matching 1 to 1 relation of the segmented CPA with the reference CPA

	Total number of 1:1 match	Total reference CPA	Correctly segmented CPAs
Geo-Eye	101	130	77.6%
Worldview-2	67	90	74.4%

An example of overlying reference segments to the automatic segmented polygons are shown in Figure 13. The red line polygon represents the manually delineated reference polygons and the polygons in blue are segmented polygons.

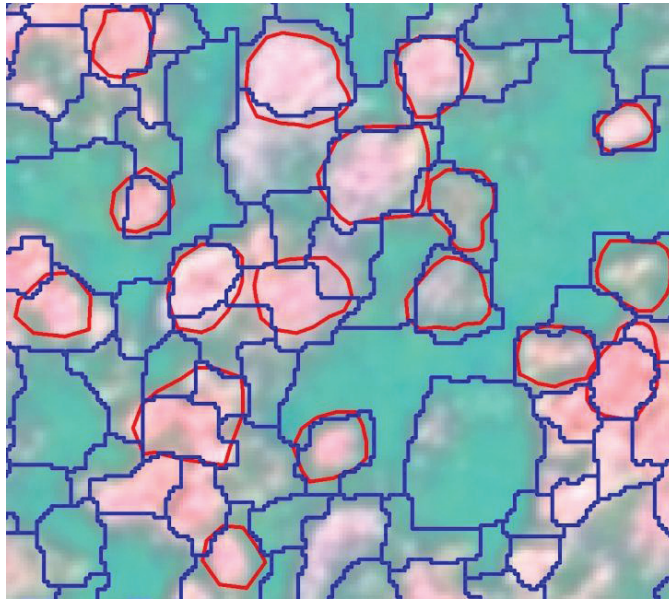


Figure 13: Visual evaluation of manual segments versus automatic segmentation of Geo-Eye image

4.2. Image classification

Image classification was done with HPF (high pass filter resolution merge) fused image (Figure 14) and classified into 2 main classes. Classification was done using Nearest Neighbourhood classification algorithm in eCognition.

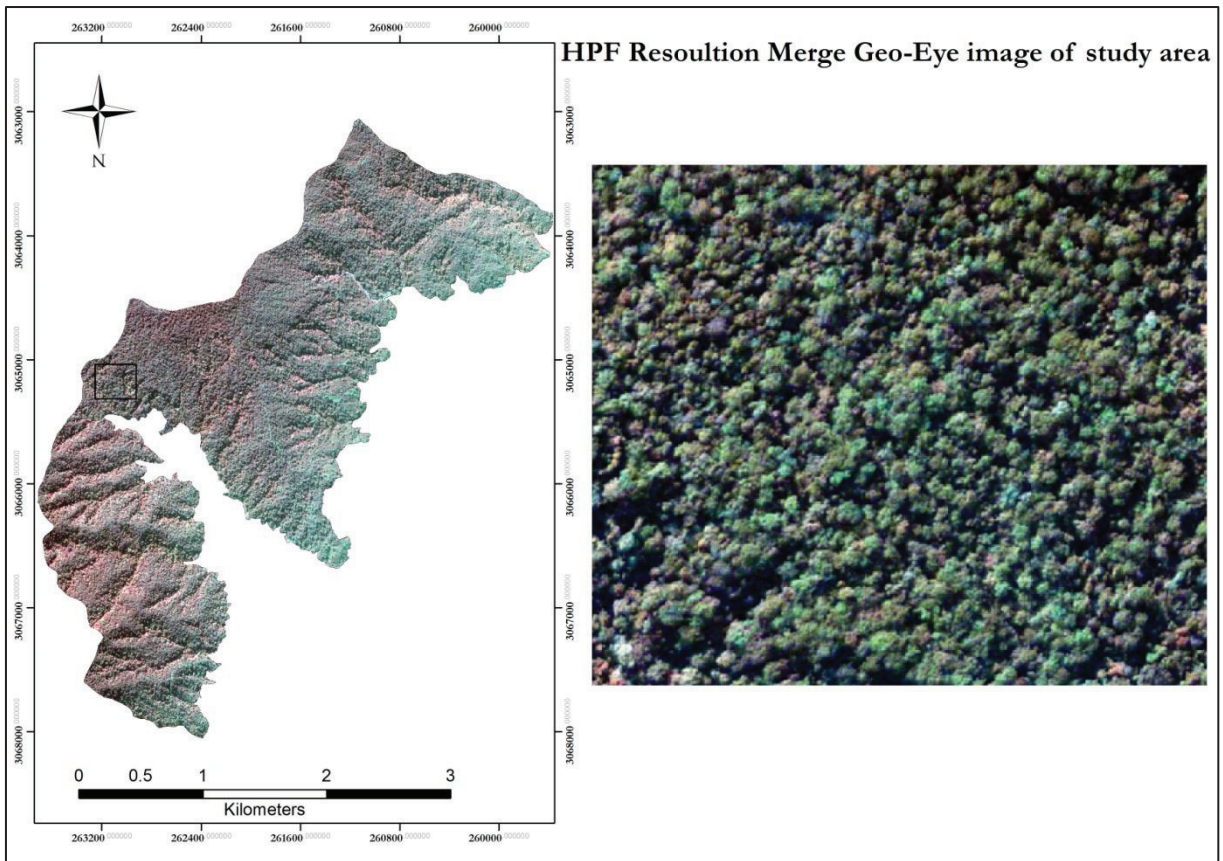


Figure 14: Fused Geo-Eye image (Inset: zooming into tree level)

4.2.1. Transformed divergence

Before classification, transformed divergence was carried out to help in distinguishing different classes. Table 6, shows that the average divergence 1506.74 in Geo-Eye image, implying the moderate separation between the species. It shows the separability in *Shorea robusta* is highest with other species, moderate separability with *Semicarpous anacardium* but it has some confusion with *Terminalia sps*, with 1161.92 divergence. *Semicarpous anacardium* on the other hand has moderately good separability with all the species. *Terminalia* species has confusion with other species and *Shorea robusta*. Thus the overall separability is good except for *Terminalia* species.

Table 6: Transformed divergence of Geo-Eye image

Signature name	Others	<i>Shorea robusta</i>	<i>Terminalia sps</i>	<i>Semicarpus anacardium</i>
Others				
<i>Shorea robusta</i>	1823.54			
<i>Terminalia sps</i>	1150.79	1161.92		
<i>Semicarpous anacardium</i>	1752.24	1506.25	1645.72	
Best average separability : 1506.74				

The transformed divergence of Worldview image is shown in Table 7. It shows the average separability of this image is better than the Geo-Eye image. The average separability obtained here is 1802.23 which is regarded to have good separation between the classes. The table shows *Semicarpous anacardium* has the best separability with all the other classes. The separability of *Shorea robusta*, *Terminalia* species, and others are moderate.

Table 7: Transformed divergence of Worldview image

Signature name	Others	<i>Shorea robusta</i>	<i>Terminalia species</i>	<i>Semicarpus anacardium</i>
Others	0			
<i>Shorea robusta</i>	1514.03	0		
<i>Terminalia sps</i>	1690.68	1611.85	0	
<i>Semicarpous anacardium</i>	1997.68	1999.53	1999.63	0
Best average separability: 1802.23				

Though the separability of *Semicarpous anacardium* is high, it is not regarded as separate class due to lack of sufficient observations to classify the images. Since the number of samples for *Shrorea robusta* was highest it was regarded as one class and all other species were merged to one classes “others”. Thus classification was done with two classes in Worldview image and an attempt was made to classify 3 species in Geo-Eye image.

4.2.2. Spectral means of the classes in every band

The spectral separability mean DN values of major species according to each band were carried out to decide on the number of classes to be made in classified image. The species which had highest number of observations were used in to derive the separability curve as shown in Figure 15 and 16. Figure 15 shows the spectral separability of four classes in Geo-Eye image. *Shorea robusta* was distinct from rest of the species. *Termianalia* species and other species were difficult to separate, so they were classified in the same class. Though *Semicarpous* species showed distinct character and was separated in the infra-red band, due to

lack of adequate observations, it was also merged with others and *Terminalia* to form single class. Shorea showed highest reflectance in both the cases and had large number of observations so, final classification was done with two classes.

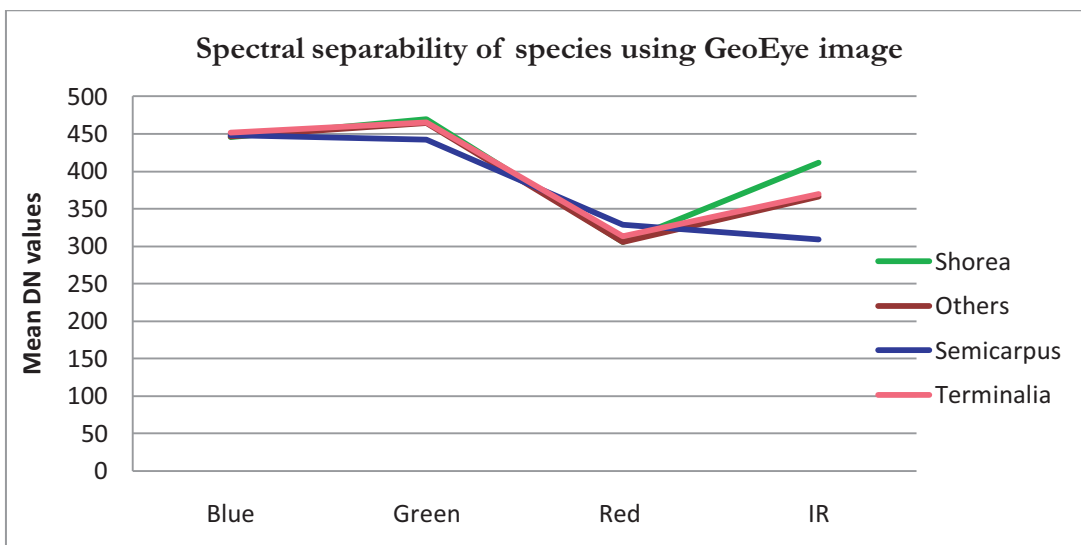


Figure 15: Spectral separability of species using GeoEye image

Similarly, Figure 16 shows the spectral separability of species into four classes and it shows that separation between the classes is higher in red edge and infra-red bands compared to the visible bands. But because of lack of sufficient number of observations, only 2 classes were made in image classification of both the images.

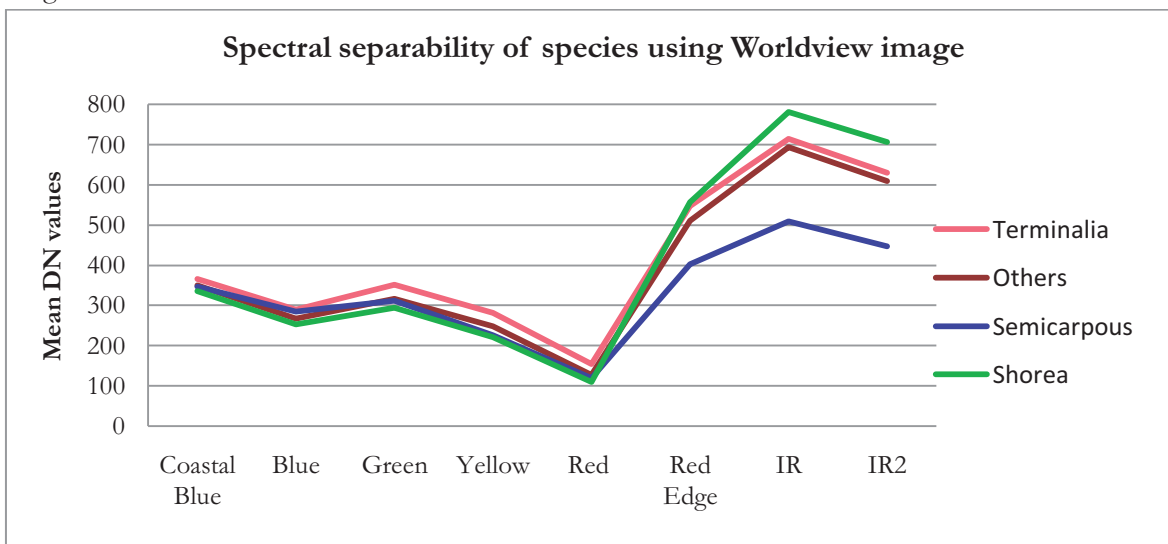


Figure 16: Spectral separability of species using Worldview image

4.2.3. Classification accuracy of Geo-eye

The classification result of Geo-Eye was validated using 38 observations 26 for *Shorea robusta* and 12 observations for other species. From confusion matrix, the classification was assessed based on the Overall accuracy, User’s accuracy, Producer’s accuracy as shown in Table 8. It shows the error matrix for classification of two classes in Geo-Eye image. It shows that 21 *Shorea robusta* observations are correctly classified as *Shorea robusta* while 4 of them are misclassified as others. Similarly in case of other species, 7 of

them are correctly classified and 5 of them are wrongly classified as *Shorea robusta*. *Shorea robusta* was most correctly identified as well as correctly classified with both the producers and users with an accuracy of 80.8%. The other class species was classified with 58.3% producers' accuracy and 63.6% users' accuracy. The overall accuracy of the classification accounted for 73.7% with two species classification. The classification result was then used to produce classification map of the study area as shown in Figure 17. The Kappa value obtained in this classification was 0.48 which is moderate value for class separation.

Table 8: Accuracy assessment of classification with two species using Geo-Eye image

Class Name	Reference Data		Classified Totals	Error of Commission (%)	Users Accuracy (%)
	<i>Shorea robusta</i>	Others			
<i>Shorea robusta</i>	21	5	26	19.2	80.8
Others	4	7	11	36.4	63.6
Totals	26	12	38		
Error of Omission (%)	15.4	41.7			
Producer's accuracy (%)	84.6	58.3			
Overall Classification Accuracy = 73.7%					

Classification using three different species using *Shorea robusta*, *Semecarpous anacardium* and others were also classified but due to lack of adequate sample data collected in the field and lack of species wise allometric equation, only two class classifications was done. Overall accuracy of the classification was 67.57% with 3 classes.

4.2.4. Classification accuracy of Worldview-2 image

In classification of Worldview image out of 100 observations, 30 of them were used for validation of the classification. The error matrix in table 9 shows that out of 19 observations of *Shorea robusta*, 13 of them were correctly classified and 5 of them were classified as other species and 1 was misclassified as shadow. In case of other species, out of 11 observations 7 of them were correctly classified as other species and 4 of them confused with *Shorea robusta*.

The overall accuracy of the Worldview classified image was 66.67% as shown in the Table 9. The producer's accuracy in case of *Shorea robusta* was 68.42% and users' accuracy of 76.47%, while in case of other species producers' accuracy is 63.64% and users' accuracy is only 58.33%. In both the classes the producers' accuracy and users accuracy was very low compared with Geo-Eye image. The Kappa value for Worldview image was only 0.32. The classification map of Worldview image is shown in Figure 18.

Table 9: Accuracy assessment of classification with two classes in Worldview

Class Name	Reference Data		Totals	Error of Commission (%)	Users Accuracy (%)
	<i>Shorea robusta</i>	Others			
Shadow	1	0	1		
<i>Shorea robusta</i>	13	4	17	23.5	76.5
Others	5	7	12	41.7	58.3
Total	19	11	30		
Error of Omission (%)	31.6	36.4			
Producer's accuracy (%)	68.4	63.6			
Overall Classification Accuracy = 66.7%					

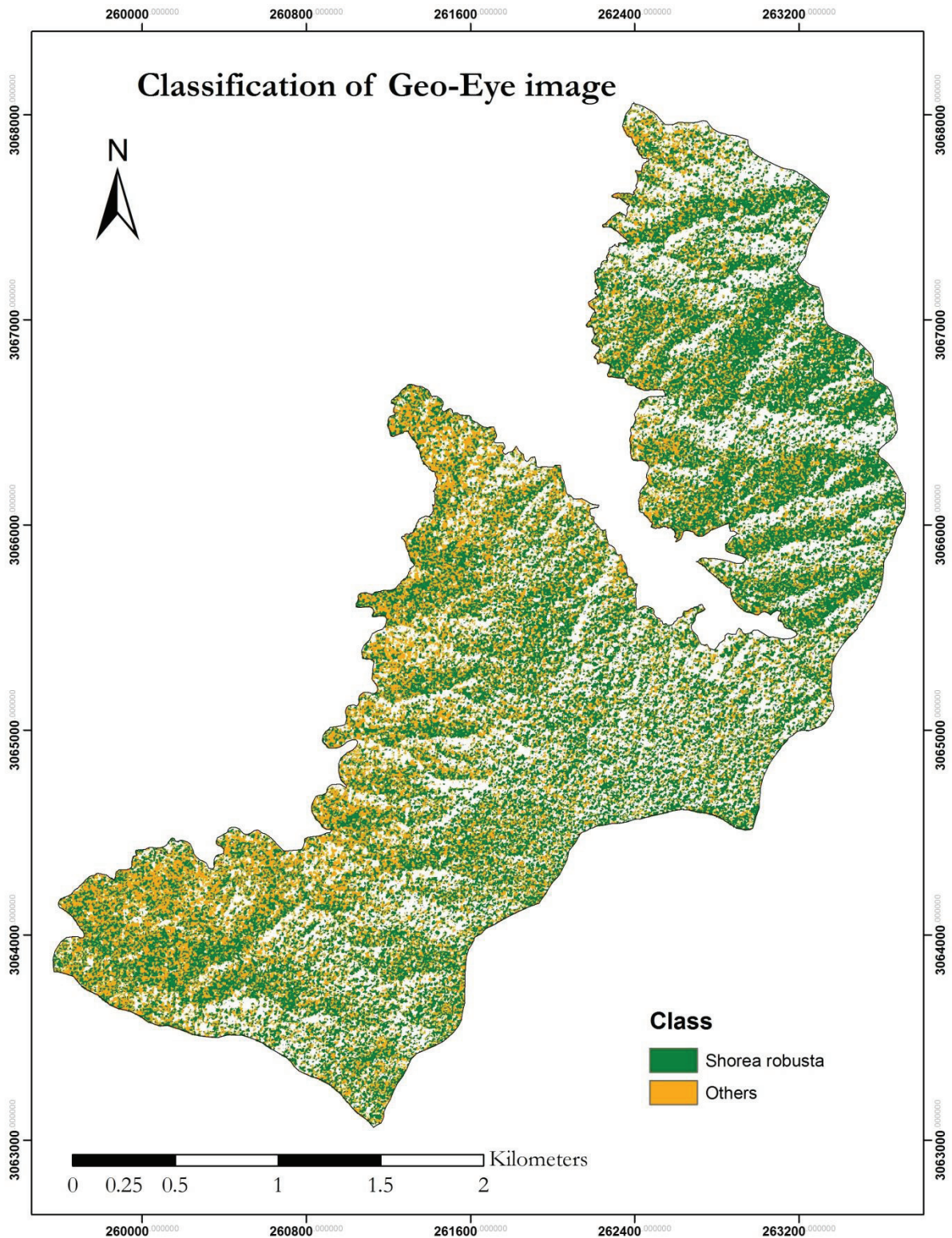


Figure 17: Classified map of Geo-Eye image

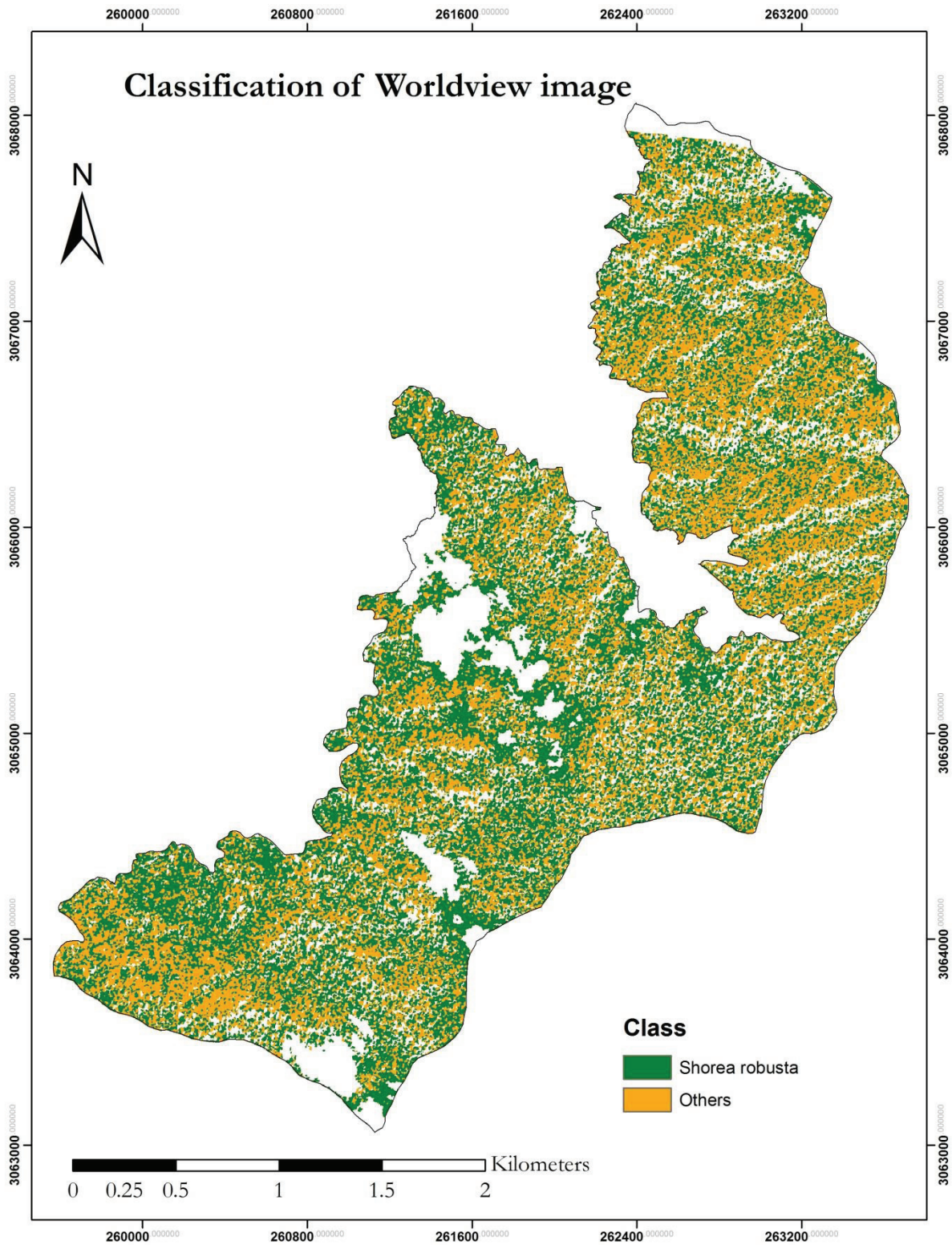


Figure 18: Classified map using Worldview

4.3. Descriptive Statistics

Altogether samples from 31 plots were collected in five CFs (Appendix-4). 749 trees were measured and total of 149 trees were recognized in the field. The distribution of the plots in the CFs is given in the Table 10. Devidhunga CFUG was the largest CF among all and had highest number of plots with 200 trees inventoried and 43 recognized. Satkanya CF was the smallest one with 4 sample plots and 123 trees were measured out of which only 20 trees could be identified.

Table 10: Forest inventory

Name of CF	Total trees inventoried	Recognized trees	No of plots
Devidhunga CF	200	43	9
Dharapani CF	169	34	8
Kalika CF	115	24	5
Kankali CF	142	28	5
Satkanya CF	123	20	4
Total	749	149	31

Chitwan is blessed with species diversity which is shown in Figure 19. *Shorea robusta* is the dominant tree species in the study area with presence of 67% occurrence followed by *Semecarpus anacardium* which is only 6% and *Terminalia tomentosa* to be 5%. There are many other species occurring less than 1% and grouped together to form a class as others which contributed to 8%.

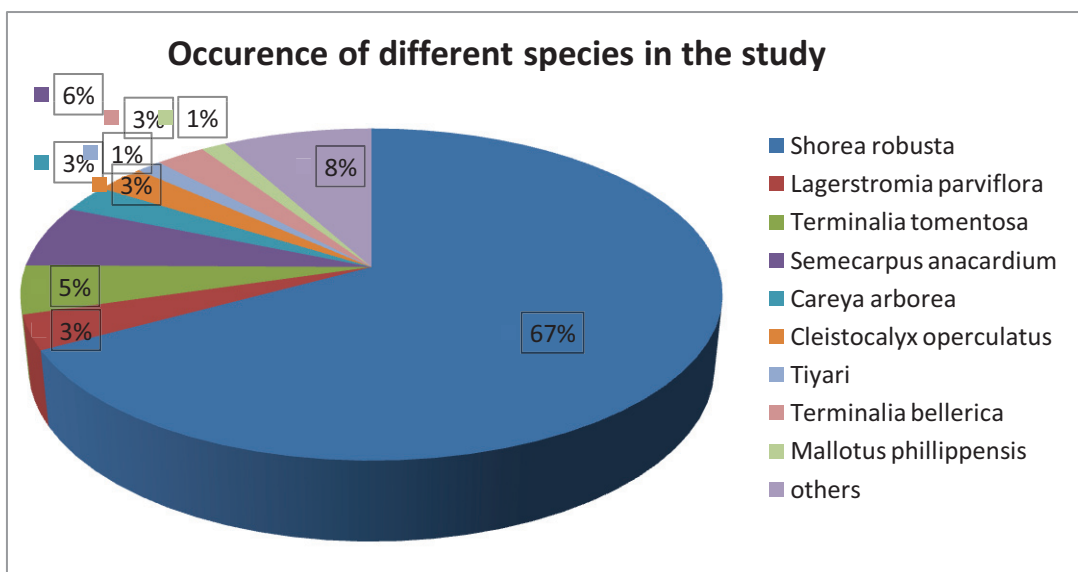


Figure 19: Species composition in the study area

DBH measured in the field was analysed using box plot (Figure 20). As can be seen from the box-plots below, the average DBH of *Shorea robusta* is more than that of other species. *Shorea robusta* has the average DBH of about 50 cm while other species has average DBH of approximately 30 cm.

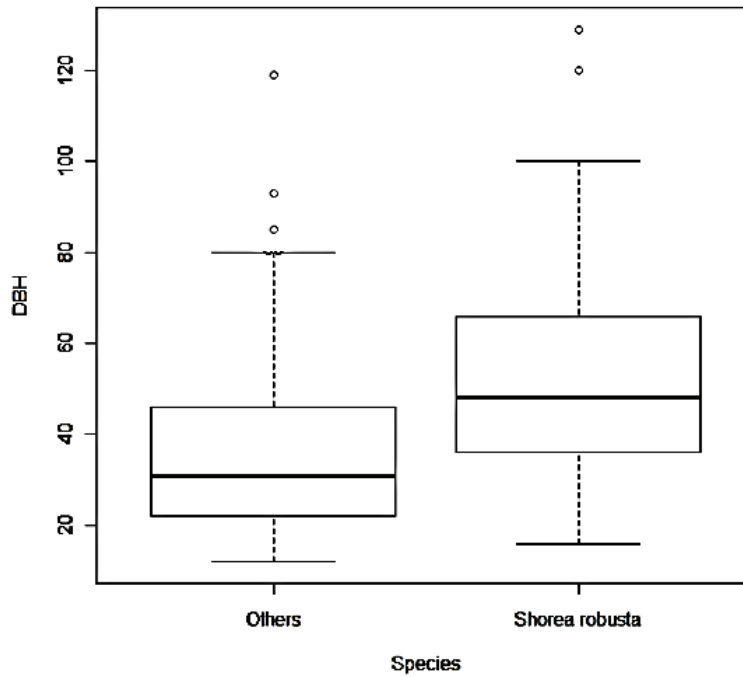


Figure 20: Box plot of the DBH of the trees measured in the field.

4.4. Model development and validation

4.4.1. Relationship between CPA and Carbon of *Shorea robusta*

Both linear and non-linear regression (Quadratic) models were developed for *Shorea robusta*. Non-linear model was preferred to simple linear regression as it predicted negative carbon values. Non-linear regression analysis was done to test if there is a relationship between CPA and Carbon. Regression was done using 32 observations for model development (Table 11). The coefficient of determination obtained in the regression model was 0.65 ($R^2=0.65$). The regression analysis also showed high correlation between CPA and Carbon as the coefficient correlation was 80 % for *Shorea robusta* (Figure 21).

Table 11: Regression Analysis of *Shorea robusta*

	Coefficients	Standard Error	t Stat	P-value
Intercept	-54.78	423.71	-0.12	0.89
CPA	5.21	13.16	0.39582	0.69
CPA ²	0.11	0.09	1.191915	0.24

One way ANOVA was employed to test the significance of Coefficient of determination- R^2 and results in the Table 12 shows that the regression was significant at 95% level of confidence.

Table 12: ANOVA test results of other species

	df	SS	MS	F	Significance F
Regression	2	6625153.473	3312577	27.39160538	2.08E-07
Residual	29	3507086.351	120934		
Total	31	10132239.82			

So, the model developed for carbon stock estimation in *Shorea robusta* is given in equation 1

$$\text{Carbon Stock} = -54.78 + 5.21 \cdot \text{CPA} + 0.11 \cdot \text{CPA}^2 \dots \dots \dots \text{eq}^n 1$$

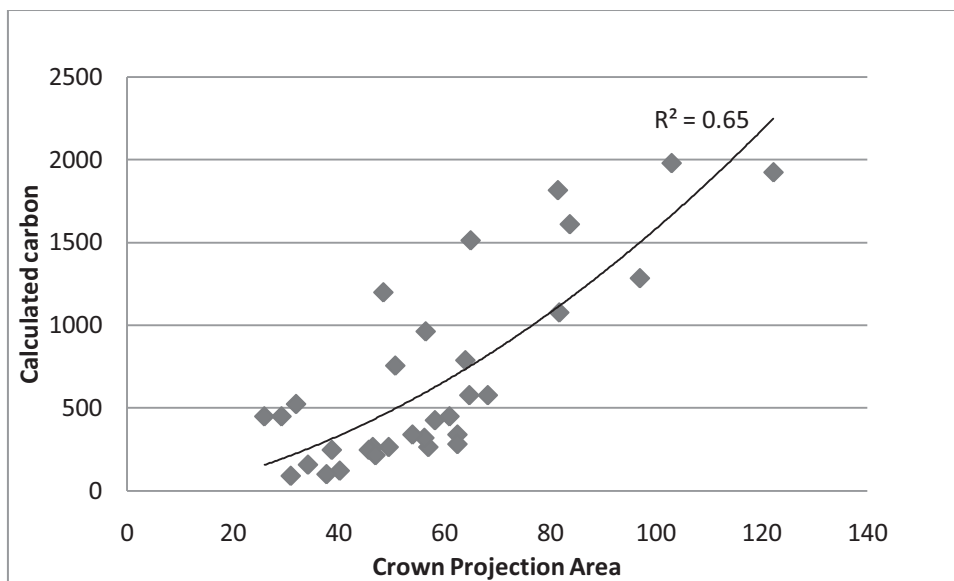


Figure 21: Graph showing the non-linear relationship between CPA and Carbon

4.4.2. Relationship between CPA and Carbon of other species

Non-linear Regression (Table 13) was done using 32 other species observations, out of which 21 were used for model development and 12 for model validation. The relationship between CPA and Carbon was found to be significant at 95% confidence level. The correlation coefficient for relationship between CPA and Carbon was higher in case of other species ($R = 0.94$) (Figure 22). The slope coefficients were from the same source so they were not significant. The coefficient of determination was 0.8 meaning that there is an agreement between CPA and Carbon of Other species. Carbon here is kg/tree and CPA is measured in m^2 .

Table 13: Non-Linear Regression analysis of other species

	Coefficients	Standard Error	t Stat	P-value
Intercept	104.38	518.17	0.20	0.84
CPA	-5.49	13.87	-0.39	0.69
CPA2	0.19	0.08	2.40	0.02

One way ANOVA was employed to test the significance of Coefficient of determination- R^2 and results in the Table 14 shows that the non-linear regression model was significant.

Table 14: ANOVA test results of other species

	df	SS	MS	F	Significance F
Regression	2	12794069	6397035	67.7697	7.94E-09
Residual	17	1604693	94393.73		
Total	19	14398763			

So, the model developed for class other species is shown in equation 2.

$$\text{Carbon} = 104.38 - 5.49 \cdot \text{CPA} + 0.19 \cdot \text{CPA}^2 \dots \dots \dots \text{eqn-2}$$

The model is fitted by non-linear regression model.

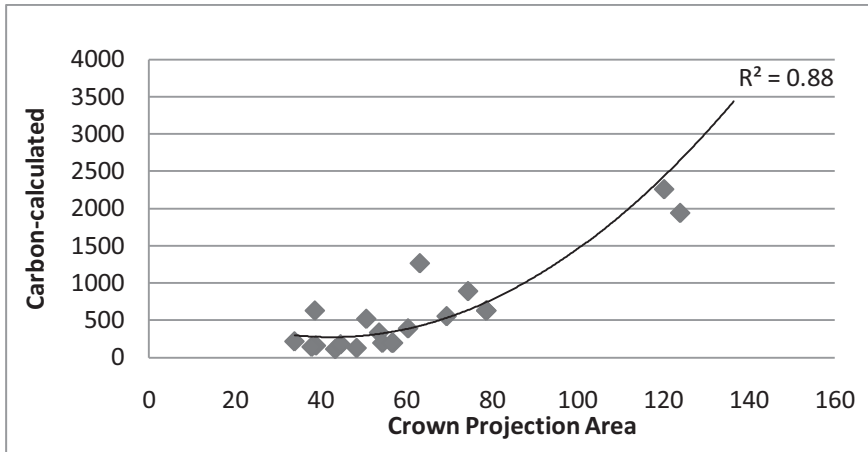


Figure 22: Scatter plot of non-linear relationship between CPA and Carbon of Other species

4.4.3. Model validation

The predicted values were plotted against calculated carbon stock. The model was validated using 14 points in case of *Shorea robusta* (Figure 23) which resulted in R² of the model validation is 0.77, meaning that 77% of the calculated carbon from the field was explained by the predicted carbon using the non-linear regression model. The test of goodness of fit was done using RMSE percentage, which resulted in 39.5%.

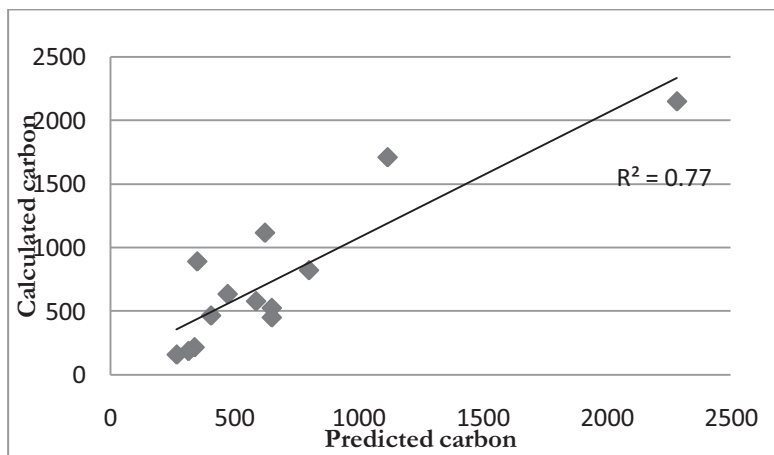


Figure 23: Scatter plot of model validation of *Shorea robusta*

Similarly, 12 points were used to validate the model in case of other species (Figure 24). The model resulted in R² of 0.79, meaning that the 79% of the calculated carbon from the field was explained by predicted carbon using this model. The test of goodness of fit was done using RMSE of this validation is 39.6%. The distribution of the validation points is not uniform in this case as most of the trees belonging to other species class were small while few trees were big.

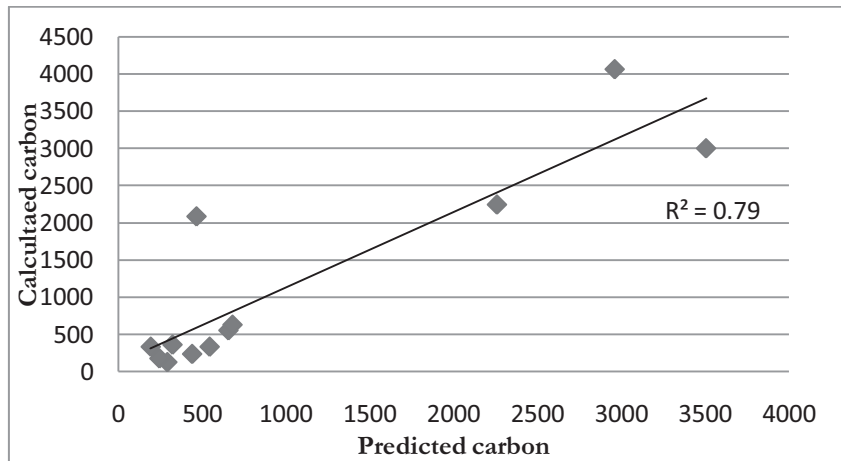


Figure 24: Scatter Plot of model validation for other species

4.5. Carbon Stock mapping

Non-linear regression model which was validated was used to estimate the amount of carbon stock in the study area. Models developed for *Shorea robusta* and other species were used for mapping *Shorea robusta* and other species. Total of 54375011 kg of carbon was estimated in the study area which covered area of 664.66 ha thus the study area has approximately 70 MgCha⁻¹. The carbon map produced here suffers from various uncertainty occurred due to error incurred in classification and segmentation. The carbon map thus produced is shown in Figure 25. Most of the trees had less than 500kg/tree carbon stock and few big trees had carbon stock more than 2000kg/tree.

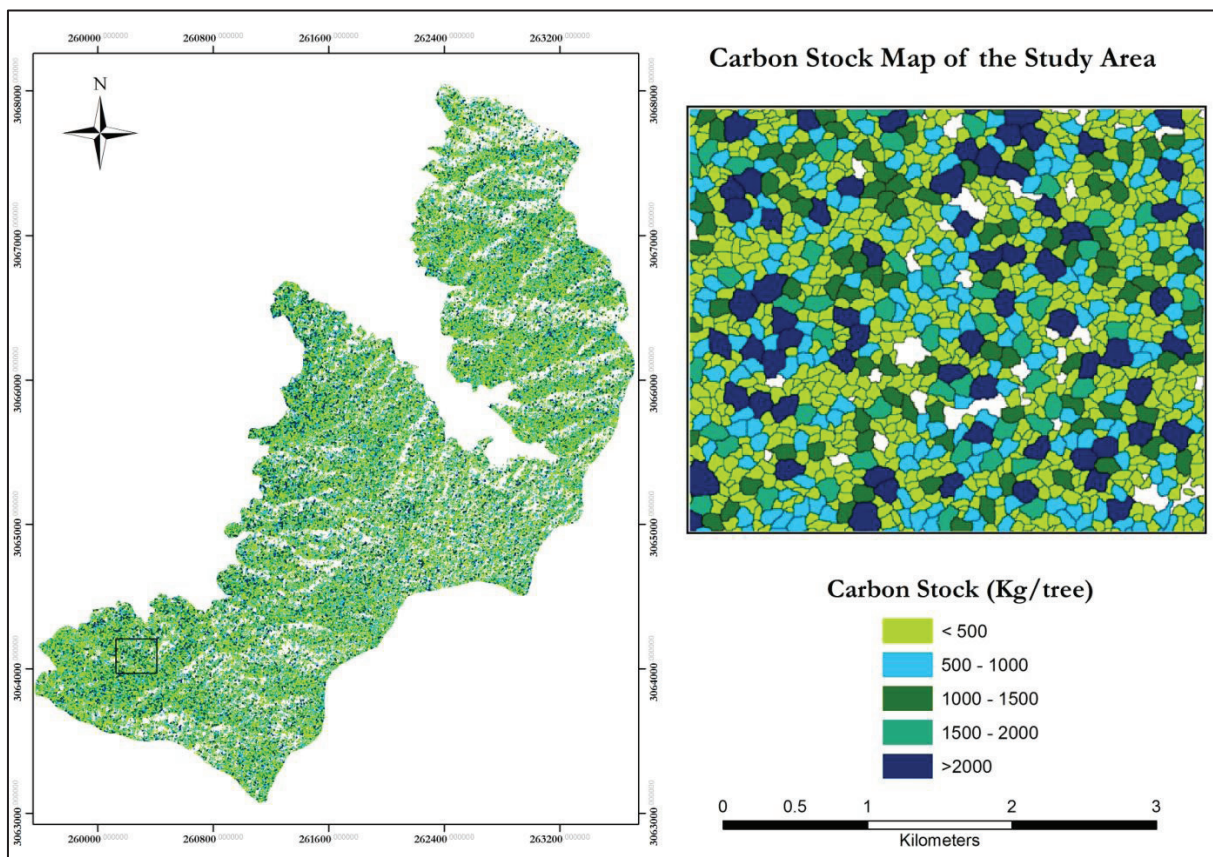


Figure 25: Carbon stock map of the study area and the inset shows the details of carbon stock per tree crown

5. DISCUSSION

5.1. Image segmentation and accuracy assessment

Accuracy assessment of segmentation for individual tree crown delineation was obtained by one to one matching of manually delineated reference polygons to automatic segments. One to one matching of the segments resulted in 77.6 % accuracy in Geo-Eye and 74.4% in Worldview image. Though the study was conducted in natural sub-tropical forest, yet the segmentation accuracy was relatively high which was expected as the segmentation evaluation was based on the positional accuracy of the reference segment to the automatic segment *i.e.* if there was overlap of at least 50% between the reference and automatic segments then the segmentation was regarded as correctly classified as done by Zhan, *et al.*, (2005). This rule was also applied in our study.

This results of segmentation accuracy achieved in this study is similar to Wang, *et al.*, (2004) who obtained 75.6% segmentation accuracy while separating tree crowns from non-crown segments. Ke & Quackenbush (2008) obtained segmentation accuracy of only 61.3% using region growing algorithm in a mixed forest of broadleaf and needle leaf trees.

Because of its capability to segment highly heterogeneous forest, multi-resolution segmentation was preferred to other individual tree crown segmentation approaches. Other individual tree crown delineation algorithms consider the trees to have conical shape (Ke & Quackenbush, 2008) and treetop to be the brightest point of the tree (Culvenor, 2002; Gonzalez, *et al.*, 2010; Leckie, *et al.*, 2005; Wang, *et al.*, 2004). This is an ideal situation occurring in managed plantation forest and segmentation done in an image acquired with less than 15° viewing angle (Wang, *et al.*, 2004). But Chitwan (study area) is complex natural forest with mixed species and age gradation. So, the issue of intermingling situation, unique branching, and illumination variation within and between crowns in natural broadleaf forest cannot be addressed by these algorithms. Hence, Multi-resolution segmentation is regarded as better option for segmentation of heterogeneous forest as tree crowns are formed based on grouping of spatially and spectrally similar pixels. Lamonaca, *et al.*, (2008) discovered that multi-resolution segmentation is successful in segmenting spatially heterogeneous forest to extract information of forest structural attributes.

The segmentation accuracy using multi-resolution segmentation depends on the scale parameter. It determines the maximum heterogeneity in the image (Kim, *et al.*, 2008). Benz *et al.*, (2004) classified the scale parameters into: fine scale, medium scale and coarse scale. Fine scale is used for extraction of trees, buildings and roads, medium scale is used for aggregated group of trees and group of buildings and coarse scale is used at land-scape level. In accordance with this, fine scale- 19 and 21 were respectively used for Geo-Eye and Worldview to extract individual trees in this study.

5.2. Image classification using Geo-Eye and Worldview-2 images

The classification accuracy achieved in this study gives moderate results with classification accuracy of 73.6% in Geo-Eye and 66.7% in Worldview image. Obtaining user's accuracy of 63.64% and 58.33% on classifying other species in Geo-Eye and Worldview image respectively implies that there is high probability that the class others in map does not represent other species on the ground. However, the user's accuracy for *Shorea robusta* was relatively high with 80.77% and 76.47% respectively for Geo-Eye and

Worldview image. The reason for high user's accuracy of *Shorea robusta* is because approximately 70% of the trees recognized in the field were *Shorea robusta*. Low user's accuracy in classifying other species is mainly attributed by the fact that there only few samples for training and validation of the results. Apart from this different species with variation in spectral characteristics had to be grouped together to form a single class which introduced confusion in the spectral response from the class 'other'.

The overall classification accuracies of the images are comparable with Erikson (2004) who obtained 77% accuracy with four species classes using less than 10 cm spatial resolution images. Key, *et al.* (2001) obtained overall accuracy of 75% on classifying four species using multi-temporal and multispectral CIR images. Gougeon & Leckie, (2006) achieved 53% overall classification accuracy on classifying six species but the accuracy was 67% when classifying two classes only. The overall classification accuracy of Worldview image are poor compared to Geo-eye and this was not expected as the image has greater spectral resolution with two infrared and red-edge band which are said to be beneficial for biomass study (DigitalGlobe, 2009). This has also been shown from few samples taken to obtain transform divergence. The average D_T was higher in case of Worldview as shown in Table 6 and Table 7. The D_T of Worldview shows high separability among the species whereas; Geo-Eye shows only moderate separability. The probable reasons for low accuracies with Worldview-2 image are discussed in detail in section 5.2.1.

The classification accuracy is also hindered by the season of image acquisition. Both the image were acquired during autumn season (October- November), which showed variation in colour within the species too. Though Hill, *et al.*, (2010) and Key, *et al.*, (2001) reported mid- autumn to be the best time for species mapping in temperate situation *i.e.* when all the trees have fully coloured. But Chitwan falls in subtropical region, which has different leaf fall season for different species. The visual inspection of the image showed that some species had changed their colour as a response to the change in season, while other species had normal colour, thus affecting the classification accuracy.

Apart from this, the spatial resolution of images (50 cm) was too coarse to detect fine details between species creating difficulties in distinguishing the reflectance from leaves of individual species. The potentiality of classifying individual tree crowns according to species is high if the spatial resolution of the image used is up to 10cm (Erikson, 2004).

5.2.1. Probable reasons for low segmentation and classification accuracy of worldview images

Geo-referencing of Worldview-2 image did not match with that of Geo-Eye image and the shapefiles of the watershed, due to this distortion in the image, identifying and locating the trees was difficult leading to low accuracy of Worldview image classification. This type of distortion in the image is unsystematic. So, classification accuracy of Worldview image was poor. The images provided in both the case were already ortho-rectified so this problem of image distortion could not be solved.

Viewing angle was 25° off-nadir in case of Worldview while it was only 15° for Geo-Eye image which makes the tree canopy to appear differently and causes confusion for the algorithm in eCognition to recognize the tree. Off nadir viewing changes the size of crown projection area on the image and this problem was also observed by Song, *et al.*, (2010), so the segmentation and classification accuracy of Worldview image was lower than that of Geo-Eye.

As observed by Song, *et al.*, (2010), time lag between the two images acquisition may add to poor classification accuracy of Worldview image. Since the worldview image was lately available and not available during the fieldwork, the trees recognition was based on the Geo-Eye image and tree recognition in worldview image was difficult as well as susceptible to errors.

Various uncertainties like cloud and huge light shadow casted by cloud were also adding in low classification accuracy of Worldview image apart from this there is also distortion in the image as shown in Figure 26. The priority of algorithm used for individual tree crown using eCognition on visualization of the image, the software did not perform well due to poor visualisation of Worldview-2 image. eCognition was unable to classify the trees behind light shadow casted by crowns.

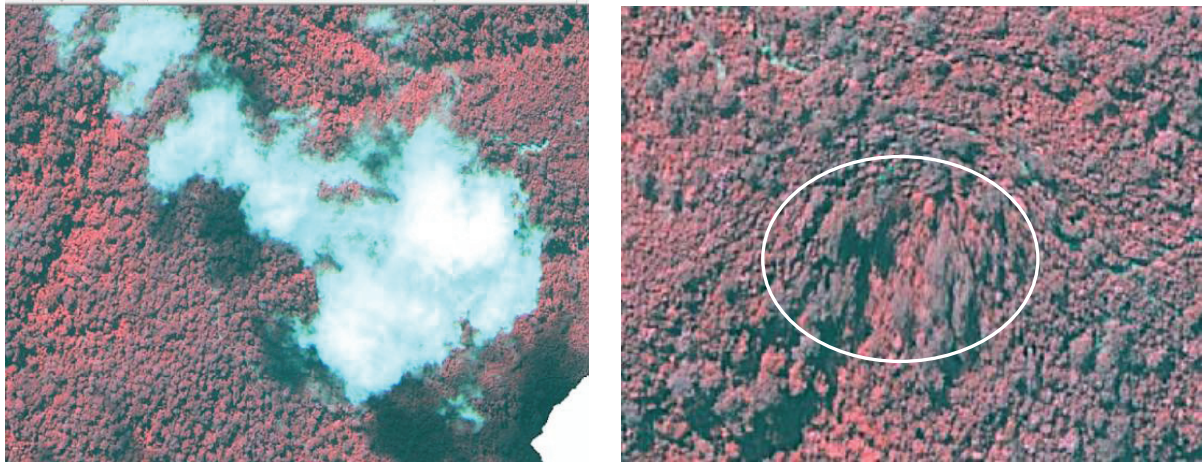


Figure 26: a) Worldview image with cloud and lot of cloud shadow b) Distortion in Worldview image

5.3. Model Development

Non-linear regression (Quadratic) equation was preferred to simple linear regression because in natural conditions also tree growth does not follow a linear relationship between diameter and the crown area in dominant forest (Kuuluvainen, 1991 (Köhl, *et al.*, 2006)). More importantly the coefficient of determination (R^2) was high using non-linear model compared to that of simple linear regression model. Besides, using non-linear regression model does not yield any negative values of carbon where as simple linear regression could only predict the carbon for CPA more than 30 m² area.

Especially in dense and diverse natural forest of Chitwan, (ANSAB, 2010) linear relationship between DBH and crown width cannot be observed with the trees with DBH larger than 40 cm (Hemery, *et al.*, 2005). Similarly in the forest with natural conditions where high competition between the species occur the relationship between DBH and CPA is non-linear (Shimano, 1997) as the tree grows, the rate of increase in CPA slow down because of competition with neighboring trees. But stem continues to grow until the tree dies though at slower rate of increase but CPA will start stabilizing and become constant after diameter has increased sufficiently (Shimano, 1997). Hence CPA starts to stabilize so does the carbon stock at lower rate due to increase in competition. In a study done on Norwegian spruce by Kuuluvainen (1991), a non-linear relationship was observed between crown projection area of dominant trees with above ground biomass. He found that the total above ground biomass accumulated in all trees faster than linearly with varying rate of increase in crown projected area.

The coefficient of determination of the models developed in the study was 0.65 for *Shorea robusta* and 0.8 for other species which is comparable with the result obtained by Hirata (2008). He established an allometric relationship between tree crown area derived from Quickbird image and DBH measured in the

field. The coefficient of determination obtained was 80%, which is comparable to other species in this research too.

The limitation of the model is that it was developed from the DBH between 10 cm to 129 cm, so the model though fits well or predicts well within this range it may produce extrapolation errors when applied beyond the range of model development data (Anderson, *et al.*, 2000).

Apart from this the validation model (Figure 24) of the other class gives the impression of clustering of the trees. It is expected as some the trees are big hardwood trees with large crowns like in case of *Terminalia tomentosa*, *Schima wallichii*, *Adina cordifolia*. But some of the trees like *Semicarpous anacardium*, *Cleistocalyx operculatus* are small trees with less carbon compared to the big trees. Thus, the clustering of the observation occurs and it could be avoided by developing species wise models rather than merging all different kinds of species in one class. Moreover, only 12 points were used for validation, if larger dataset was used, error and fitness of the model would have been improved.

5.4. Biomass and Carbon stock estimation

The results of this research shows that the carbon stock of the study area was approximately 70 Mg Cha⁻¹ which is comparable with the results of Kaul (2010) who calculated the carbon sequestration rate of few species of India including *Shorea robusta* and found that it contains 82 Mg Cha⁻¹, which was the largest carbon stock among other species studied. The result is poorer compared to Baral *et al.*, (2009) who obtained 96.6 Mg Cha⁻¹ in a study done in Chitwan district, Nepal. This is mainly because the models developed in this study can predict only 61% of carbon estimates.

5.5. Sources of error or uncertainties

5.5.1. Shadows causing error in high resolution satellite images.

As both the images had large solar angle of 46° and 45°, respectively for Worldview and Geo-Eye images, the persistence of inter-crown shadow in the images is obvious (Andersson, *et al.*, 2009; Gonzalez, *et al.*, 2010; Wulder, White, *et al.*, 2004). Morales *et al.*, (2009) explained the poor accuracy of their segmentation was because of shadow which was also the case in this study. The poor the poor accuracy of CPA derivation was because of shadow. Shadow is even a bigger problem when the forest is dense with closed canopy. The presence of shadow in the image often obscures the regular pattern of the trees which negatively affected the identification of tree tops as they sometimes confuse with branches also as tree tops especially in the dense tropical forest. Similar was the case with Gonzalez,(2010) where shadows were casted up to 25 m long that hindered the ability of the automated crown detection algorithm not only to accurately locate tree tops and but also locate trees with relatively smaller crowns. Asner (2002) made an attempt to avoid the crown shadow problem by manually tracing the trees but manual crown delineation is not possible for researches in large areas as well in dense forest (Gonzalez, *et al.*, 2010). With increasing the scale parameters for segmentation, the issue of shadow can be decreased but at some point the objects become larger than a single forest stand and which causes decreasing classification accuracy (Ke, *et al.*, 2010). This solution provided by Ke *et al.*, (2010) cannot be applied in this case as the forest which is very diverse in terms of species composition as well as age. Similarly, Zhengrong (2008) suggested in decreasing the resolution of the image to reduce the shadow effect but this method makes tree crown boundary to be less distinct and make the delineation difficult.

Similarly the shadows in the image do not allow the whole tree to be displayed properly as few pixels of the tree are under shadow as shown in Figure 27, so this problem has also significant error in classifying

the high resolution images. In his review article for biomass estimation Lu (2006) summarized that high resolution satellite images possess the drawback of having large amount of shadow which in itself is an obstacle in developing biomass estimation models. Shadows in high resolution satellite images seriously affects the quality of the image as it causes loss of information from the features because of false colour tone and distortion in shape of the object (Haijian, *et al.*, 2008).

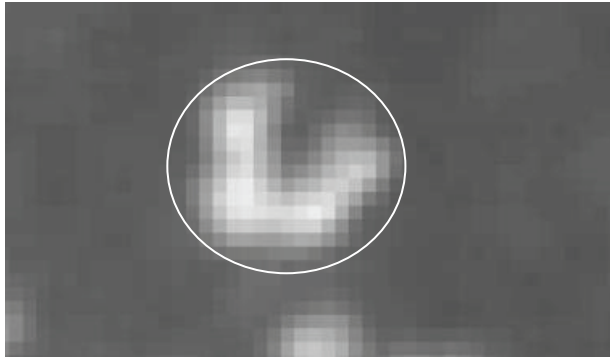


Figure 27: Missing pixels of a tree because of shadow

5.5.2. Allometric equations

The uncertainty related with allometric equations is that general allometric equation does not include variation in site quality like age, soil type, climate, stand structure and genetic properties *etc.* (Kuuluvainen, 1991). These variations in site qualities are the peculiarities that persist in tropical and sub-tropical forests.

The general allometric equation used in the study uses the diameter as the predictable variable. Even in very diverse forest DBH alone explains more than 95% of the variation in aboveground carbon stocks in tropical forest (Andersson, *et al.*, 2009). But biomass is not only affected by DBH but also by height and wood density (Basuki, *et al.*, 2009). So, this introduces error in estimation of carbon stock.

The coefficient parameters “a” and “b” in allometric equations are the major sources of uncertainty as they are not calibrated for individual sites (Ketterings, *et al.*, 2001). So, these coefficients are useful in estimating these parameters in stands where they are investigated (Zianis & Mencuccini, 2004) but extrapolating these values to other regions is erroneous.

Similarly, using general allometric equation also encounters error in tree measurement, sampling uncertainty and representativeness of the network of small plots over vast forest landscape (Chave, *et al.*, 2004). They are constructed from limited samples and specific gravity of wood is not taken into consideration.

The allometric equation used in this research are from different sources, the allometric equation used for *Shorea robusta* is developed by Basuki, *et al.*, (2009) for Indonesia. This equation was preferred to IPCC general equation because the mean temperature of researcher’s study area are similar with Indonesia having mean annual temperature of 26°C and that of Chitwan, Nepal was 25°C. The rainfall of Chitwan was approximately 1500 mm/ yr. which was similar to 2000mm/yr. in Indonesia. Apart from this the sampling was intensive taking the diameter range of 6 cm to 200 cm to develop the model (Basuki, *et al.*, 2009)

5.5.3. Time of image acquisition

The Geo-Eye image was acquired on November 2009 and fieldwork was carried out on September 2010 while Worldview image was obtained only after the fieldwork. The worldview image used in the study was acquired in October, 2010. The tree crown during the field work may be slightly bigger than in Geo-Eye image because of the growth season in between (Song, *et al.*, 2010).

5.6. Limitations of the research

5.6.1. Intermingling situation in the natural forest

Species intermingling is an issue in image segmentation and classification, even small scale differences in canopy spectral properties tends to generate different spectral signatures (Lamonaca, *et al.*, 2008). But this issue is beyond the scope of this research.

5.6.2. Sampling design

One of the limitations of the research was number of sampling plots and recognized trees to develop the method. The strategy for sampling was initially developed for the whole study area and later when the size of study area was reduced, the numbers of samples available for analysis were limited. This is also the limitation of eCognition as it could not handle a big dataset and study area was made small.

5.6.3. Undergrowth not addressed by the model

The tree detection and delineation algorithms that are available cannot detect the undergrowth of forest (Palace, *et al.*, 2008). The suppressed trees which are covered by dominant trees are not considered in the study as they are not seen by the sensor.

6. CONCLUSION AND RECOMMENDATIONS

Using high resolution satellite images are found to be advantageous in segmentation and classification. Significant relationship between CPA and Carbon was observed which will be making carbon stock estimation more convenient using remote sensing technique accompanied by field work.

6.1. Conclusions

1. Related to research question 1, **“Segmentation using different spectral resolution images”**

The segmentation accuracy was not so different using different spectral resolution images. Though Geo-Eye image with four bands performed better than eight band Worldview image, the slight higher segmentation accuracy was because of geo-referencing problem of Worldview image. The segmentation accuracy was assessed by matching the manually delineated CPA with segmented CPA. The segmentation accuracy of Geo-Eye was 77.6 % and that of Worldview was 74.4%.

2. Related to research question 2, **“Classification accuracy using different spectral resolution images”**

The classification using Geo-Eye image yield better results in this case compared to Worldview image. The spectral separability curve and transformed divergence showed the potentiality to obtain higher classification accuracy from Worldview image but due to distortions and artefacts overall classification accuracy of Worldview was poor compared to GeoEye image. The overall classification accuracies of Geo-Eye and Worldview are 73.6% and 66.7% respectively with two classes.

3. Related to research question 3, **“The relationship between CPA and Carbon stock”**

There exists a reasonable non-linear relationship between CPA derived from Geo-Eye image and Carbon stock obtained from DBH measured in the field. The coefficient of determination of 0.65 for *Shorea robusta* and 0.88 for other species indicate that there exists a strong relationship between CPA and carbon stock. The model validation results showed that *Shorea robusta* had coefficient of determination of 0.77 and other class had 0.79. The predicted carbon stock obtained from these models suffered from RMSE of 39%, which implies that models could predict carbon with only 61% accuracy. If the number of validation points were more than the error in the model would have improved.

4. Related to research question 4, **“Carbon stock in the study area”**

The total amount of carbon stock in the study area was 54375 Mg which was approximately 70 MgCha⁻¹.

Related to general objective “method developed to estimate the carbon stock using high resolution satellite images”

The relationship between CPA and DBH was found to be significant at 95% confidence level. Quadratic model was found to explain the relationship with 39% RMSE. Though the model developed suffers from high error percentage it is feasible to estimate the amount of carbon stock using high resolution satellite

images with some improvements. Improvements can be made on developing species wise model with abundant number of samples. Both Worldview and Geo-Eye image has ample opportunities to be used in carbon stock estimation.

6.2. Recommendations

The method developed in this study suffers from high accuracy, thus there are certain things that should be improved before using this method to estimate the carbon stock based on CPA-DBH relationship. Firstly there should be sufficient number of observations/ samples for each species. Having sufficient samples will be helpful to develop species wise CPA-DBH models which will certainly add to reduce the error in the model.

Due to lack of local level allometric equation, general allometric equation and equation developed for Indonesia were used. The error will certainly reduce if local allometric equations are used for carbon stock estimation. Thus, development of local level allometric equations for Nepal is required for better carbon stock estimation.

Moreover, forest in sub-tropical regions like Chitwan is fast growing and diverse, where intermingling and overlapping situation exists between the canopies of different trees. So, study on intermingling situation will be better to get more accurate estimation of carbon stock from crown projection area.

Besides Worldview image has 8 spectral bands which has good separability within species resulted in poor classification accuracy due problem in geo-referencing and other artefacts. It is highly recommended to use this image for further exploration to estimate the amount of carbon stock.

LIST OF REFERENCES

- Acharya, K. P. (2002). Twenty-four years of community forestry in Nepal. *International Forestry Review*, 4(2), pp 149–156.
- Acharya, K. P., Dangi, R. B., Tripathi, D. M., Bushley, B. R., Bhandary, R. R., & Bhattarai, B. (2009). *Ready for REDD: Taking Stock of Experience, Opportunities and Challenges in Nepal*: Nepal Foresters' Association.
- Alves, L. F., & Santos, F. A. M. (2002). Tree allometry and crown shape of four tree species in Atlantic rain forest, south-east Brazil. *Journal of Tropical Ecology*, 18, pp 245-260.
- Amolins, K., Zhang, Y., & Dare, P. (2007). Wavelet based image fusion techniques - An introduction, review and comparison. [Review]. *ISPRS Journal of Photogrammetry and Remote Sensing*, 62(4), pp 249-263.
- Amro, I., & Mateos, J. (2010). Multispectral image pansharpening based on the contourlet transform. *Journal of Physics: Conference Series*, 206(1).
- Anderson, S. C., Kupfer, J. A., Wilson, R. R., & Cooper, R. J. (2000). Estimating forest crown area removed by selection cutting: a linked regression-GIS approach based on stump diameters. *Forest Ecology and Management*, 137(1-3), pp 171-177.
- Andersson, K., Evans, T., & Richards, K. (2009). National forest carbon inventories: policy needs and assessment capacity. *Climatic Change*, 93(1), pp 69-101.
- ANSAB. (2010). *Report on forest carbon stocks in Ludikhola, Kayarkhola and Charnawati Watersheds of Nepal Forest Carbon Stock in REDD+ Pilot Project Sites: Year One Measurement & Analysis*. Kathmandu, Nepal
- Asner, G. P., Palace, M., Keller, M., Jr.Rodrigo, P., Silva, J. N. M., & Zweede, J. C. (2002). Estimating Canopy Structure in an Amazon Forest from Laser Range Finder and IKONOS Satellite Observations. *BIOTROPICA*, 34(4).
- Asner, G. P., Palace, M., Keller, M., Pereira, R., Silva, J. N. M., & Zweede, J. C. (2002). Estimating canopy structure in an Amazon Forest from laser range finder and IKONOS satellite observations. *Biotropica*, 34(4), pp 483-492.
- Baral, S. K., Malla, R., & S, R. (2009). Above-ground carbon stock assessment in different forest types of Nepal. *Banko Jankari*, 19(2), pp 10-14.
- Basuki, T. M., van Laake, P. E., Skidmore, A. K., & Hussin, Y. A. (2009). Allometric equations for estimating the above-ground biomass in tropical lowland Dipterocarp forests. *Forest Ecology and Management*, 257(8), pp 1684-1694.
- Benz, U. C., Hofmann, P., Willhauck, G., Lingenfelder, I., & Heynen, M. (2004). Multi-resolution, object-oriented fuzzy analysis of remote sensing data for GIS-ready information. *ISPRS Journal of Photogrammetry and Remote Sensing*, 58(3-4), pp 239-258.
- Blaschke, T. (2010). Object based image analysis for remote sensing. *ISPRS Journal of Photogrammetry and Remote Sensing*, 65(1), pp 2-16.
- Blaschke, T., Burnett, C., & Pekkarinen, A. (2004). *Image Segmentation Methods for Object-based Analysis and Classification*. In S. M. D. Jong & F. D. V. d. Meer (Eds.), *Remote Sensing Image Analysis: Including The Spatial Domain*: Springer Netherlands. (Vol. 5), pp. 211-236.
- Boggs, G. S. (2010). Assessment of SPOT 5 and QuickBird remotely sensed imagery for mapping tree cover in savannas. *International Journal of Applied Earth Observation and Geoinformation*, 12(4), pp 217-224.
- Brown, S. (2002). Measuring carbon in forests: current status and future challenges. *Environmental Pollution*, 116(3), pp 363-372.
- Bunting, P., Lucas, R. M., Jones, K., & Bean, A. R. (2010). Characterisation and mapping of forest communities by clustering individual tree crowns. *Remote Sensing of Environment*, 114(11), pp 2536-2547.
- Cardoso, J. S., & Corte-Real, L. (2005). Toward a generic evaluation of image segmentation. *IEEE Transactions on Image Processing*, 14(11), pp 1773-1782.
- Carleer, A. P., Debeir, O., & Wolff, E. (2005). Assessment of very high spatial resolution satellite image segmentations. *Photogrammetric Engineering and Remote Sensing*, 71(11), pp 1285-1294.
- Castilla, G., & Hay, G. J. (2008). *Image objects and geographic objects*. In T. Blaschke, S. Lang & G. J. Hay (Eds.), *Object-Based Image Analysis*, Springer Berlin Heidelberg. (pp. 91-110).
- Chapagain, N., & Banjade, M. R. (2009). Community Forestry and Local Development: Experiences from the Koshi Hills of Nepal. *Journal of Forest and Livelihood*, 8 ((2)). Kathmandu.

- Chave, J., Condit, R., Aguilar, S., Hernandez, A., Lao, S., & Perez, R. (2004). *Error propagation and scaling for tropical forest biomass estimates*. Royal Society of London.
- Chavez, P. S., Sides, S. C., & Anderson, J. A. (1991). Comparison Of 3 Different Methods To Merge Multiresolution and Multispectral Data- Lansat TM and Spot Panchromatic. *Photogrammetric Engineering and Remote Sensing*, 57(3), pp 295-303.
- Chubey, M. S., Franklin, S. E., & Wulder, M. A. (2006). Object-based analysis of Ikonos-2 imagery for extraction of forest inventory parameters. *Photogrammetric Engineering and Remote Sensing*, 72(4), pp 383-394.
- Cole, W. G., & Lorimer, C. G. (1994). Predicting tree growth from crown variables in managed northern hardwood stands. *Forest Ecology and Management*, 67(1-3), pp 159-175.
- Culvenor, D. S. (2002). TIDA: an algorithm for the delineation of tree crowns in high spatial resolution remotely sensed imagery. *Computers & Geosciences*, 28(1), pp 33-44.
- Culvenor, D. S. (2003). *Extracting individual tree information: a survey of techniques for high spatial resolution imagery*. In M. A. e. Wulder & S. E. e. Franklin (Eds.), *Remote sensing of forest environments : concepts and case studies*. Boston Kluwer Academic. (pp. 255-277)
- Definiens. (2009a). *Definiens eCognition Developer 8 Reference Book*.
- Definiens. (2009b). *Definiens eCognition Developer 8 User Guide*.
- Dhital, N. (2009). Reducing Emissions from Deforestation and Forest Degradation (REDD) in Nepal: Exploring the Possibilities. *Journal of Forest and Livelihoods*, 8 (1).
- DigitalGlobe. (2009). WHITE PAPER The Benefits of the 8 Spectral Bands of WorldView-2. from <http://www.digitalglobe.com/index.php/88/WorldView-2>
- Drăguț, L., Tiede, D., & Levick, S. R. (2010). ESP: a tool to estimate scale parameter for multiresolution image segmentation of remotely sensed data. *International Journal of Geographical Information Science*, 24(6), pp 859 - 871.
- Dubayah, R. O., & Drake, J. B. (2000). Lidar remote sensing for forestry. *Journal of Forestry*, 98(6), 44-46.
- Erikson, M. (2004). Species classification of individually segmented tree crowns in high-resolution aerial images using radiometric and morphologic image measures. *Remote Sensing of Environment*, 91(3-4), pp 469-477.
- Faganaa, M., & DeFries, R. (2009). *Measurement and Monitoring of the World's Forests A Review and Summary of Remote Sensing Technical Capability, 2009–2015*. 1616 P Street NW, Washington, DC 20036: Resources for Future.
- FAO. (2008). Forests and climate change Better forest management has key role to play in dealing with climate change. Retrieved 15 August 2010, from <http://www.fao.org/newsroom/en/focus/2006/1000247/index.html>
- FAO. (2010, Tuesday, July 27, 2010). Global forest resource assessment 2010 country report Nepal. Retrieved 15 August, 2010, from http://www.forestrynepal.org/images/publications/fra_2010_nepal.pdf
- GeoEye.(2010). Retrieved 12/22/2010, from <http://www.geoeye.com/CorpSite/products-and-services/imagery-collection/Default.aspx>
- Gibbs, H. K., Brown, S., Niles, J. O., & Foley, J. A. (2007). Monitoring and estimating tropical forest carbon stocks: making REDD a reality. *Environmental Research Letters*, 2(4).
- Gibbs, H. K., & Herold, M. (2007). Tropical deforestation and greenhouse gas emissions. *Environmental Research Letters*, 2(4).
- Gonzalez, P., Asner, G. P., Battles, J. J., Lefsky, M. A., Waring, K. M., & Palace, M. (2010). Forest carbon densities and uncertainties from Lidar, QuickBird, and field measurements in California. *Remote Sensing of Environment*, 114(7), pp 1561-1575.
- Gougeon, F. A., & Leckie, D. G. (2006). The individual tree crown approach applied to Ikonos images of a coniferous plantation area. *Photogrammetric Engineering and Remote Sensing*, 72(11), pp 1287-1297.
- Greenberg, J. A., Dobrowski, S. Z., & Ustin, S. L. (2005). Shadow allometry: Estimating tree structural parameters using hyperspatial image analysis. *Remote Sensing of Environment*, 97(1), pp 15-25.
- Gschwantner, T., Schadauer, K., Vidal, C., Lanz, A., Tomppo, E., di Cosmo, L., et al. (2009). Common Tree Definitions for National Forest Inventories in Europe. [Review]. *Silva Fennica*, 43(2), pp 303-321.
- Haijian, M., Qiming, Q., & Xinyi, S. (2008, 7-11 July 2008). *Shadow Segmentation and Compensation in High Resolution Satellite Images*. Paper presented at the Geoscience and Remote Sensing Symposium, 2008. IGARSS 2008. IEEE International.

- Hay, G. J., Blaschke, T., Marceau, D. J., & Bouchard, A. (2003). A comparison of three image-object methods for the multiscale analysis of landscape structure. *ISPRS Journal of Photogrammetry and Remote Sensing*, 57(5-6), pp 327-345.
- Hay, G. J., Castilla, G., Wulder, M. A., & Ruiz, J. R. (2005). An automated object-based approach for the multiscale image segmentation of forest scenes. *International Journal of Applied Earth Observation and Geoinformation*, 7(4), pp 339-359.
- Hemery, G. E., Savill, P. S., & Pryor, S. N. (2005). Applications of the crown diameter-stem diameter relationship for different species of broadleaved trees. *Forest Ecology and Management*, 215(1-3), pp 285-294.
- Hill, R. A., Wilson, A. K., George, M., & Hinsley, S. A. (2010). Mapping tree species in temperate deciduous woodland using time-series multi-spectral data. *Applied Vegetation Science*, 13(1), pp 86-99.
- Hirata, Y. (2008). Estimation of stand attributes in *Cryptomeria japonica* and *Chamaecyparis obtusa* stands using QuickBird panchromatic data. *Journal of Forest Research*, 13(3), pp 147-154.
- Hirata, Y., Tsubota, Y., & Sakai, A. (2009). Allometric models of DBH and crown area derived from QuickBird panchromatic data in *Cryptomeria japonica* and *Chamaecyparis obtusa* stands. *International Journal of Remote Sensing*, 30(19), pp 5071 - 5088.
- Hunt, C. A. G. (2009). *Carbon sinks and climate change : forests in the fight against global warming : e-book*. Cheltenham: Edward Elgar.
- Husch, B., Beers, T. W., & Kershaw, J. A. (2003). *Forest mensuration* (Fourth edition.). Hoboken: Wiley & Sons.
- IPCC. (2006). 2006 IPCC Guidelines for National Greenhouse Gas Inventories Volume 4 Agriculture, Forestry and Other Land Use Retrieved 19 August 2010, from http://www.ipcc-nggip.iges.or.jp/public/2006gl/pdf/4_Volume4/V4_04_Ch4_Forest_Land.pdf
- IPCC. (2007a). Good Practice Guidance for Land Use, Land-Use Change and Forestry. from http://www.ipcc-nggip.iges.or.jp/public/gpگلulucf/gpگلulucf_contents.html
- IPCC. (2007b). Summary for Policymakers. In: Climate Change 2007: The Physical Science Basis. Contribution of Working Group I to the Fourth Assessment Report of the Intergovernmental Panel on Climate Change. Retrieved 8 August 2010
- Jennings, S. B., Brown, N. D., & Sheil, D. (1999). Assessing forest canopies and understorey illumination: Canopy closure, canopy cover and other measures. *Forestry*, 72, pp 59-73.
- Jensen, J. R. (1986). *Introductory digital image processing : a remote sensing perspective*. Englewood Cliffs: Prentice-Hall.
- Joshi, J. R. (2010). *Improving the quality of digital surface model generated from very high resolution satellite stereo imagery by using object oriented image analysis technique*. Unpublished Msc Thesis, University of Twente Faculty of Geo-Information and Earth Observation ITC, Enschede.
- Kasischke, E. S., Melack, J. M., & Craig Dobson, M. (1997). The use of imaging radars for ecological applications--A review. *Remote Sensing of Environment*, 59(2), pp 141-156.
- Katoh, M., Gougeon, F., & Leckie, D. (2009). Application of high-resolution airborne data using individual tree crowns in Japanese conifer plantations. *Journal of Forest Research*, 14(1), 10-19.
- Kaul, M., Mohren, G. M. J., & Dadhwal, V. K. (2010). Carbon storage and sequestration potential of selected tree species in India. *Mitigation and Adaptation Strategies for Global Change*, 15, pp 489-510.
- Ke, Y., & Quackenbush, L. J. *Comparison of individual tree crown detection and delineation methods*. Paper presented at the American Society of Photogrammetry and Remote Sensing, Bethesda, Maryland, Portland, Oregon.
- Ke, Y., Quackenbush, L. J., & Im, J. (2010). Synergistic use of QuickBird multispectral imagery and LIDAR data for object-based forest species classification. *Remote Sensing of Environment*, 114(6), pp 1141-1154.
- Kerle, N. e., Janssen, L. L. F. e., Huurneman, G. C. e., Bakker, W. H., Grabmaier, K. A., Huurneman, G. C., et al. (2004). *Principles of remote sensing : an introductory textbook* (Third edition ed.). Enschede: ITC.
- Ketterings, Q. M., Coe, R., van Noordwijk, M., Ambagau, Y., & Palm, C. A. (2001). Reducing uncertainty in the use of allometric biomass equations for predicting above-ground tree biomass in mixed secondary forests. *Forest Ecology and Management*, 146(1-3), pp 199-209.
- Key, T., Warner, T. A., McGraw, J. B., & Fajvan, M. A. (2001). A Comparison of Multispectral and Multitemporal Information in High Spatial Resolution Imagery for Classification of Individual Tree Species in a Temperate Hardwood Forest. *Remote Sensing of Environment*, 75(1), pp 100-112.

- Kim, M., Madden, M., & Warner, T. (2008). Estimation of optimal image object size for the segmentation of forest stands with multispectral IKONOS imagery pp. 291-307.
- Köhl, M., Magnussen, S., & Marchetti, M. (2006). *Tropical Forestry: Sampling Methods, Remote Sensing and GIS Multiresource Forest Inventory* Springer- Verlag Berlin Heidelberg.
- Krankina, O. N., Harmon, M. E., Cohen, W. B., Oetter, D. R., Olga, Z., & Duane, M. V. (2004). Carbon Stores, Sinks, and Sources in Forests of Northwestern Russia: Can We Reconcile Forest Inventories with Remote Sensing Results? *Climatic Change*, 67(2), pp 257-272.
- Kuuluvainen, T. (1991). Relationships between crown projected area and components of above-ground biomass in Norway spruce trees in even-aged stands: Empirical results and their interpretation. *Forest Ecology and Management*, 40(3-4), pp 243-260.
- Laliberte, A. S., Koppa, J., Fredrickson, E. L., & Rango, A. (2006). *Comparison of nearest neighbor and rule-based decision tree classification in an object-oriented environment*. IEEE International Geoscience and Remote Sensing Symposium, IGARSS, July 31, 2006 - August 4, 2006, Denver, CO, United states.
- Lamonaca, A., Corona, P., & Barbati, A. (2008). Exploring forest structural complexity by multi-scale segmentation of VHR imagery. *Remote Sensing of Environment*, 112(6), pp 2839-2849.
- Leckie, D. G., Gougeon, F. A., Tinis, S., Nelson, T., Burnett, C. N., & Paradine, D. (2005). Automated tree recognition in old growth conifer stands with high resolution digital imagery. *Remote Sensing of Environment*, 94(3), pp 311-326.
- Lillesand, T. M., Kiefer, R. W., & Chipman, J. W. (2008). *Remote sensing and image interpretation* (Sixth edition ed.). New York: Wiley & Sons.
- Lu, D. (2005). Aboveground biomass estimation using Landsat TM data in the Brazilian Amazon. *International Journal of Remote Sensing*, 26(12), pp 2509 - 2525.
- Lu, D. (2006). The potential and challenge of remote sensing-based biomass estimation. [Review]. *International Journal of Remote Sensing*, 27(7), pp 1297-1328.
- MOFSC. (2009). Ministry of Forests and Soil Conservation, Government of Nepal. Retrieved 29 May 2010, from <http://mofsc-redd.gov.np/introduction/>
- Möller, M., Lymburner, L., & Volk, M. (2007). The comparison index: A tool for assessing the accuracy of image segmentation. *International Journal of Applied Earth Observation and Geoinformation*, 9(3), pp 311-321.
- Mora, B., Wulder, M. A., & White, J. C. (2010). Segment-constrained regression tree estimation of forest stand height from very high spatial resolution panchromatic imagery over a boreal environment. *Remote Sensing of Environment*, In Press, Corrected Proof.
- Morales, R. M., Miura, T., & Idol, T. (2008). An assessment of Hawaiian dry forest condition with fine resolution remote sensing. *Forest Ecology and Management*, 255(7), pp 2524-2532.
- Muukkonen, P., & Heiskanen, J. (2007). Biomass estimation over a large area based on standwise forest inventory data and ASTER and MODIS satellite data: A possibility to verify carbon inventories. *Remote Sensing of Environment*, 107(4), 617-624.
- Nagendra, H., & Rocchini, D. (2008). High resolution satellite imagery for tropical biodiversity studies: the devil is in the detail. [10.1007/s10531-008-9479-0]. *Biodiversity and Conservation*, 17(14), 3431-3442.
- Nguyen, N. T. (2010). *Estimation and mapping of above ground biomass for the assessment and mapping of carbon stocks in tropical forest using SAR data : a case study in Afram headwaters forest, Ghana*. Unpublished Msc Thesis, ITC, Enschede.
- Ojha, H., Persha, L., & Chhatre, A. (2009). *Community Forestry in Nepal : A policy innovation for local livelihoods and food security* Paper presented at the International Forestry Resources and Institutions Program, School of Natural Resources and Environment, University of Michigan
- Oli, B. N., & Shrestha, K. (2009). Carbon Status in Forests of Nepal: An Overview. *Journal of Forest and Livelihood*, 8(1) February 2009 Forest Action, Kathmandu.
- Omasa, K., Qiu, G. Y., Watanuki, K., Yoshimi, K., & Akiyama, Y. (2003). Accurate Estimation of Forest Carbon Stocks by 3-D Remote Sensing of Individual Trees. *Environmental Science & Technology*, 37(6), pp 1198-1201.
- Ozdemir, I. (2008). Estimating stem volume by tree crown area and tree shadow area extracted from pan-sharpened Quickbird imagery in open Crimean juniper forests. *International Journal of Remote Sensing*, 29(19), pp 5643-5655.
- Palace, M., Keller, M., Asner, G. P., Hagen, S., & Braswell, B. (2008). Amazon forest structure from IKONOS satellite data and the automated characterization of forest canopy properties. *BIOTROPICA*, 40(2), pp 141-150.

- Panta, M. (2003). *Analysis of forest canopy density and factors affecting it using RS and GIS techniques : a case study from Chitwan district of Nepal*. Unpublished MSc, ITC, Enschede.
- Patenaude, G., Milne, R., & Dawson, T. P. (2005). Synthesis of remote sensing approaches for forest carbon estimation: reporting to the Kyoto Protocol. *Environmental Science & Policy*, 8(2), pp 161-178.
- Pekkarinen, A., & Holopainen, M. (2006). Segmentation. In A. Kangas & M. Maltamo (Eds.), *Forest Inventory* Springer Netherlands. (10), pp. 253-269.
- Pouliot, D. A., King, D. J., Bell, F. W., & Pitt, D. G. (2002). Automated tree crown detection and delineation in high-resolution digital camera imagery of coniferous forest regeneration. *Remote Sensing of Environment*, 82(2-3), pp 322-334.
- Pretzsch, H. (2009). *Forest Dynamics, Growth and Yield: From Measurement to Model* Available from <http://books.google.com/books>. retrieved on February 1 2011.
- Rejaur, M., & Saha, S. (2008). Multi-resolution segmentation for object-based classification and accuracy assessment of land use/land cover classification using remotely sensed data. *Journal of the Indian Society of Remote Sensing*, 36(2), pp 189-201.
- Rosenqvist, Å., Milne, A., Lucas, R., Imhoff, M., & Dobson, C. (2003). A review of remote sensing technology in support of the Kyoto Protocol. *Environmental Science & Policy*, 6(5), pp 441-455.
- Shimano, K. (1997). Analysis of the relationship between DBH and crown projection area using a new model. *Journal of Forest Research*, 2(4), pp 237-242.
- Sierra, C. A., del Valle, J. I., Orrego, S. A., Moreno, F. H., Harmon, M. E., Zapata, M., *et al.* (2007). Total carbon stocks in a tropical forest landscape of the Porce region, Colombia. [Article]. *Forest Ecology and Management*, 243(2-3), pp 299-309.
- Simone, G., Farina, A., Morabito, F. C., Serpico, S. B., & Bruzzone, L. (2002). Image fusion techniques for remote sensing applications. *Information Fusion*, 3(1), pp 3-15.
- Song, C. (2007). Estimating tree crown size with spatial information of high resolution optical remotely sensed imagery.. *International Journal of Remote Sensing*, 28(15), pp 3305-3322.
- Song, C., Dickinson, M. B., Su, L., Zhang, S., & Yaussey, D. (2010). Estimating average tree crown size using spatial information from Ikonos and QuickBird images: Across-sensor and across-site comparisons. *Remote Sensing of Environment*, 114(5), pp 1099-1107.
- Steininger, M. K. (2000). Satellite estimation of tropical secondary forest above-ground biomass: data from Brazil and Bolivia. *International Journal of Remote Sensing*, 21(6), pp 1139 - 1157.
- Tan, Y. M., Huai, J. Z., & Tang, Z. S. (2010). An Object-Oriented Remote Sensing Image Segmentation Approach Based on Edge Detection. *Spectroscopy and Spectral Analysis*, 30(6), pp 1624-1627.
- Thenkabail, P. S., Enclona, E. A., Ashton, M. S., Legg, C., & De Dieu, M. J. (2004). Hyperion, IKONOS, ALI, and ETM+ sensors in the study of African rainforests. *Remote Sensing of Environment*, 90(1), pp 23-43.
- Thoms, C. A. (2008). Community control of resources and the challenge of improving local livelihoods: A critical examination of community forestry in Nepal. *Geoforum*, 39(3), pp 1452-1465.
- UNFCCC.(2011).Kyoto Protocol.Retrieved Jan 24, 2011, from http://unfccc.int/kyoto_protocol/items/2830.php
- Wang, L., Gong, P., & Biging, G. S. (2004). Individual Tree-Crown Delineation and Treetop Detection in High-Spatial-Resolution Aerial Imagery. *Photogrammetric Engineering & Remote Sensing*, 70(3), pp 351-357.
- Wei, W., Chen, X., & Ma, A. (2005). *Object-oriented information extraction and application in high-resolution remote sensing image*. Paper presented at the 2005 IEEE International Geoscience and Remote Sensing Symposium, IGARSS 2005, July 25, 2005 - July 29, 2005, Seoul, Republic of Korea.
- Wulder, M. A., Hall, R. J., Coops, N. C., & Franklin, S. E. (2004). High spatial resolution remotely sensed data for ecosystem characterization. *Bioscience*, 54(6), pp 511-521.
- Wulder, M. A., White, J. C., Niemann, K. O., & Nelson, T. (2004). Comparison of airborne and satellite high spatial resolution data for the identification of individual trees with local maxima filtering. *International Journal of Remote Sensing*, 25(11), pp 2225-2232.
- Zhan, Q., Molenaar, M., Tempfli, K., & Shi, W. (2005). Quality assessment for geo-spatial objects derived from remotely sensed data. *International Journal of Remote Sensing*, 26(14), pp 2953 - 2974.
- Zhang, Feng, X. Z., & Jiang, H. (2010). Object-oriented method for urban vegetation mapping using IKONOS imagery. *International Journal of Remote Sensing*, 31(1), pp 177-196.
- Zhang, Y., & Maxwell, T. (2006). *A Fuzzy Logic Approach To Supervised Segmentation For Object Oriented Classification*.Retrieved from <http://www.asprs.org/publications/proceedings/reno2006/0183.pdf>

- Zhengrong, L., Hayward, R., Jinglan, Z., & Yuee, L. (2008). *Individual tree crown delineation techniques for vegetation management in power line corridor*. Paper presented at the 2008 Digital Image Computing: Techniques and Applications, 1-3 Dec. 2008, Piscataway, NJ, USA.
- Zianis, D., & Mencuccini, M. (2004). On simplifying allometric analyses of forest biomass. *Forest Ecology and Management*, 187(2-3), pp 311-332.

APPENDICES

Appendix 1: Specification of the images used

Design and Specifications	World-View2	Geo-Eye1												
Launch Information	Date: October 8, 2009 Vandenberg Air Force Base, California	September 6, 2008 Vandenberg Air Force Base, California												
Orbit	Altitude: 770 kilometers Type: Sun synchronous, Period: 100 minutes	Altitude: 684 kilometers Type: Sun-synchronous Period: 98 minutes												
Mission Life	7.25 years, including all consumables and degradable (e.g. propellant)	Fully redundant 7+ year design life; fuel for 15 years												
Sensor Bands	Panchromatic 8 Multispectral: 4 standard colours: blue, green, red, near-IR 1 4 new colours: coastal, yellow, red edge, near-IR 2	Panchromatic 4 Multispectral 4 Standard colours: blue, green, red, near- IR												
Sensor Resolution (GSD = Ground Sample Distance)	Panchromatic: 0.46 meters GSD at nadir Multispectral: 1.84 meters GSD at nadir (note that imagery must be re-sampled to 0.5 meters for non-US Government customers)	Panchromatic: 0.41 m (nominal at nadir) Multispectral: 1.65 m (nominal at nadir) (note that imagery must be re-sampled to 0.5 meters for non-US Government customers)												
Swath Width	16.4 kilometres at nadir	15.2 km / 9.44 mi at nadir												
Max Viewing Angle / Accessible Ground Swath	Nominally +/-45° off-nadir = 1355 km wide swath Higher angles selectively available													
Revisit Frequency	1.1 days at 1 meter GSD or less 3.7 days at 20° off-nadir or less (0.52 meter GSD)	<table border="1"> <thead> <tr> <th>Max Pan GSD (m)</th> <th>Off Nadir Look Angle (deg)</th> <th>Average Revisit (days)</th> </tr> </thead> <tbody> <tr> <td>0.42</td> <td>10</td> <td>8.3</td> </tr> <tr> <td>0.50</td> <td>28</td> <td>2.8</td> </tr> <tr> <td>0.59</td> <td>35</td> <td>2.1</td> </tr> </tbody> </table>	Max Pan GSD (m)	Off Nadir Look Angle (deg)	Average Revisit (days)	0.42	10	8.3	0.50	28	2.8	0.59	35	2.1
Max Pan GSD (m)	Off Nadir Look Angle (deg)	Average Revisit (days)												
0.42	10	8.3												
0.50	28	2.8												
0.59	35	2.1												

Appendix 2: Data collection format

Data Collection Form

Name of recorder:

Date:

Slope:

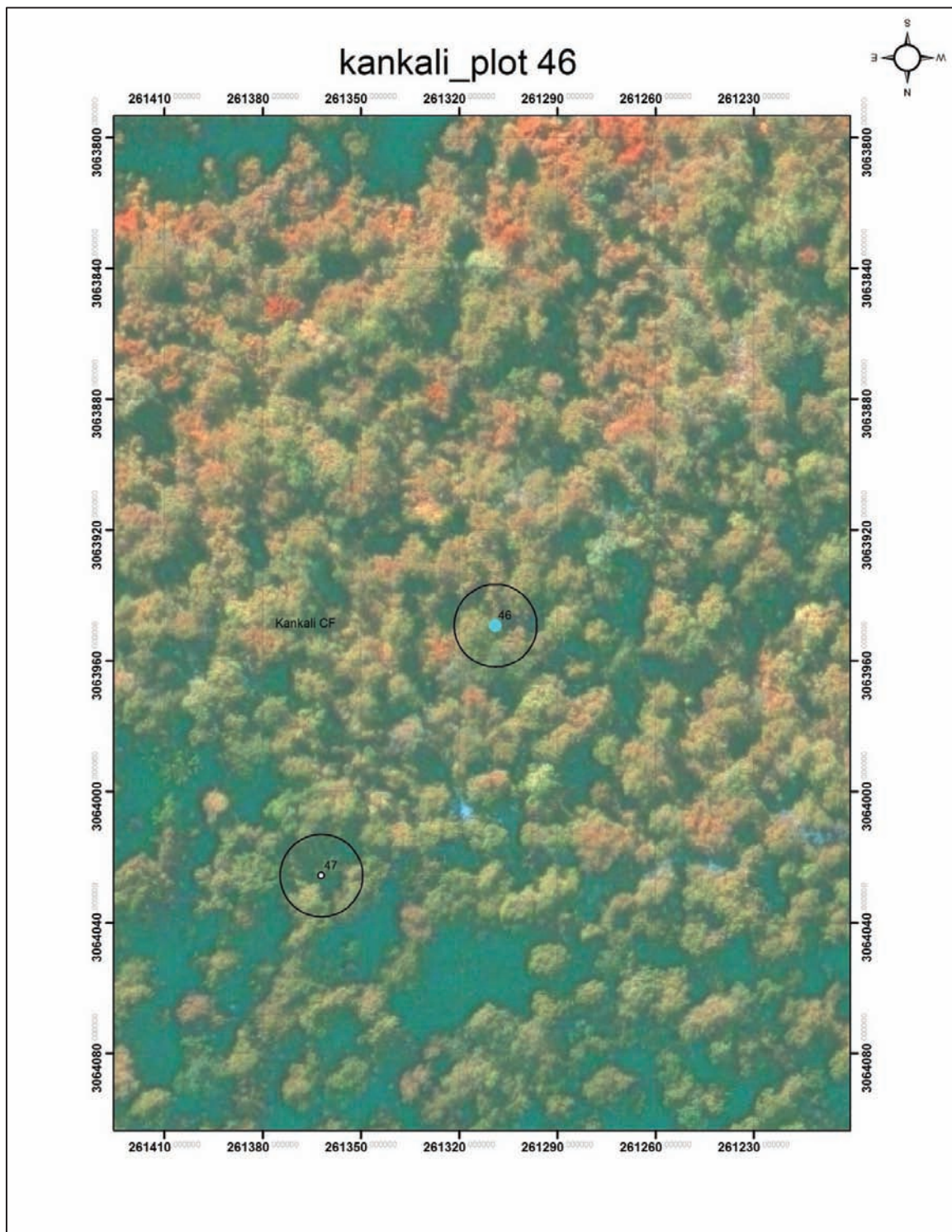
aspect:

altitude:

Stratum ID		Coordinates	X:
Sample plot ID			Y:

S.N.	Species	DB H (cm)	Crown diameter (m)	Height (m)	Remarks
1.					
2.					
3.					
4.					
5.					
6.					
7.					
8.					
9.					
10.					
11.					
12.					
13.					
14.					
15.					
16.					
17.					
18.					
19.					
20.					
21.					
22.					
23.					
24.					
25.					

Appendix 3: Map of the sample plot used for tree identification in the field



Appendix 4: Sample plots

Stratum ID	Sample plot number	X	Y
Devidhunga	1	263212	3067655
Devidhunga	2	262427	3066730
Devidhunga	3	263449	3066713
Devidhunga	4	262685	3067590
Devidhunga	5	262545	3066300
Devidhunga	6	262712	3066036
Dharapani	7	262100	3065850
Dharapani	8	261290	3065720
Dharapani	9	262173	3065452
Dharapani	10	261412	3066285
Kalika	11	261480	3065240
Kalika	12	261950	3064832
Kalika	13	261810	3065640
Kalika	14	262490	3064960
Kankali	15	259896	3063969
Kankali	16	261310	3063948
Kankali	17	261042	3064085
Kankali	18	260590	3063776
Satkanya	19	260370	3064250
Satkanya	20	261227	3064018
Kalika	21	260272	3063967
Kalika	22	261571	3063914
Satkanya	23	260571	3064386
Dharapani	24	262321	3065737
Dharapani	25	261823	3066087
Devidhunga	26	262592	3067694
Devidhunga	27	262378	3067173
Kalika	28	261756	3065280
Satkanya	29	260891	3063967
Kalika	30	261229	3064801
Dharapani	31	262861	3065139
Devidhunga	32	263114	3066150

Appendix 5: List of tree species in the study area

S.N.	Local name	Scientific name
1	Khamari	<i>Gmelia arborea</i>
2	Sal	<i>Shorea robusta</i>
3	Gausi	Vernacular name
4	Bot Dhayero	<i>Lagerstromia parviflora</i>
5	Bhalayo	<i>Semicarpous anacardium</i>
6	Harro	<i>Terminalia chebula</i>
7	Jamun	<i>Syzygium cumini</i>
8	Aci	Vernacular name
9	Ghakri syaula	Vernacular name
10	Chilaune	<i>Schima Wallichii</i>
11	Katus	<i>Castonopsis indica</i>
12	Khirro	<i>Holarrhena pubescens</i>
13	Tatari	<i>Dillenia pentagyna</i>
14	Kumvi	<i>Careya arborea</i>
15	Kande	Vernacular name
16	Barro	<i>Terminalia belerica</i>
17	Asna	<i>Terminalia tomentosa</i>
18	Bhalukath	<i>Sida rhombifolia</i>
19	Gayo	Vernacular name
20	Raj Brikshya	<i>Cassia fistula</i>
21	Barkaula	<i>Casaria graveolens</i>
22	Padke	<i>Albizia julibrissin</i>
23	Kusum	<i>Scleichiara oleosa</i>
24	Kyamuna	<i>Cleistocahyx operculatus</i>
25	Vorle	Vernacular name
26	Tiyari	Vernacular name
27	Sindure	<i>Mallotus philippensis</i>
28	Tuni	Vernacular name
29	Siris	<i>Albezia procera</i>
30	Karma	<i>Adina cordifolia</i>
31	Simal	<i>Bombax ceiba</i>

Appendix 6: Glimpse of the Chitwan

